2009

Implementing Pulse Compression in the Iwrap Airborne Doppler Radar/Scatterometer

John J. Mcmanus
University of Massachusetts Amherst

IMPLEMENTING PULSE COMPRESSION IN THE IWRAP AIRBORNE DOPPLER RADAR/SCATTEROMETER

A Thesis Presented

by

JOHN J. MCMANUS

Submitted to the Graduate School of the
University of Massachusetts Amherst in partial fulfillment
of the requirements for the degree of

MASTER OF SCIENCE IN ELECTRICAL AND COMPUTER ENGINEERING

February 2009

Electrical and Computer Engineering

IMPLEMENTING PULSE COMPRESSION IN THE IWRAP AIRBORNE DOPPLER RADAR/SCATTEROMETER

A Thesis Presented

by

JOHN J. MCMANUS

Approved as to style and content by:

Stephen J. Frasier, Chair

Paul Siqueira, Member

James Carswell, Member

C. V. Hollot, Department Chair
Electrical and Computer Engineering

ABSTRACT

IMPLEMENTING PULSE COMPRESSION IN THE IWRAP AIRBORNE DOPPLER RADAR/SCATTEROMETER

FEBRUARY 2009

JOHN J. MCMANUS

B.S.E.E., SYRACUSE UNIVERSITY

M.S.E.C.E., UNIVERSITY OF MASSACHUSETTS AMHERST

Directed by: Professor Stephen J. Frasier

The pulse compression scheme implemented on the Imaging Wind and Rain Airborne Profiler (IWRAP) is described. Developed at the UMASS Microwave Remote Sensing Laboratory (MIRSL), IWRAP is a dual-band (C and Ku) conically scanning Doppler scatterometer designed to map the atmospheric boundary layer wind fields, ocean surface wind fields, and precipitation within tropical cyclones. IWRAP has previously been deployed using a pulsed transmit waveform with a peak transmit power of 80 watts. This limits the average transmit power and sensitivity for the system which affects the more distant range gates (especially at Ku-band). As a result, IWRAP could operate only at lower altitudes (approx. 5000 ft) causing safety concerns and limiting the missions for which it can be deployed.

Increasing sensitivity was achieved by converting IWRAP to a pulse compression radar system. Pulse compression is a technique that combines the increased energy of a longer pulse with the high resolution of a short pulse by implementing a frequency

modulated (FM) "chirped" transmit waveform. This method requires advanced signal processing, in which the received signal is passed through a filter to compress the pulse on the receiving end. A system with various chirp/filtering schemes as well as a new control system which UMASS has recently developed will be discussed in this thesis.

TABLE OF CONTENTS

LIST OF TABLES

Table **Page**

LIST OF FIGURES

Figure **Page**

CHAPTER 1

INTRODUCTION

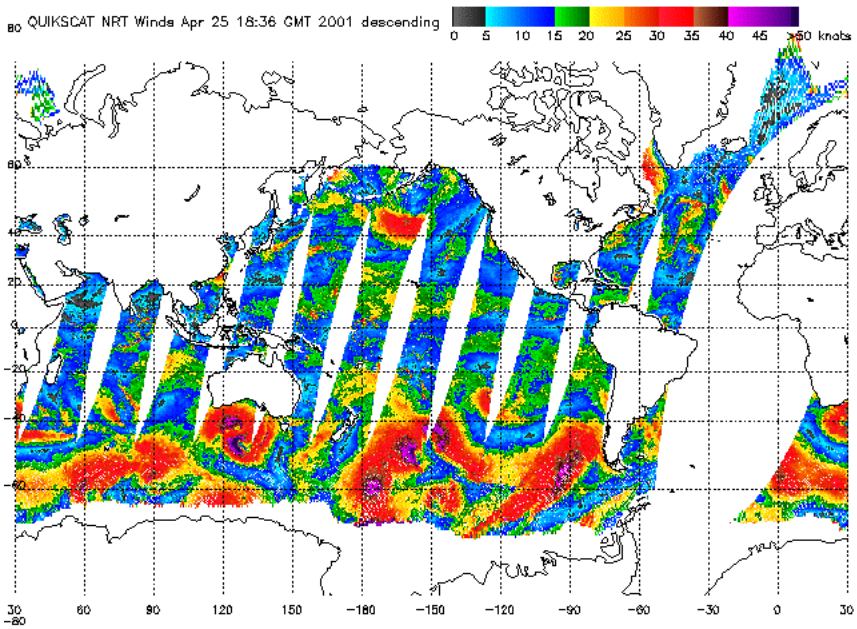

Figure 1.1. QuikSCAT wind product: Ocean surface wind field for a single day [11]

Tropical cyclones (TCs) pose a significant threat to densely populated coastal areas in and around the United States. Much of the damage caused has been a result of the high winds and rain-rate associated with TCs. For years scientists have been analyzing data from various remote sensing systems to more accurately measure near-surface ocean wind velocity and to help predict tropical cyclone intensity and track. One such remote sensing instrument is the radar scatterometer. Scatterometers are calibrated radars that transmit a known amount of energy and measure the backscatter from surfaces to determine their normalized radar cross section (NRCS, or σ_o).

Because of the sensitivity of the NRCS of ocean surface roughness, which is directly influenced by the surface wind velocity, it is feasible to estimate the ocean surface wind velocity from microwave scatterometer observations. The relationship between the ocean NRCS, rain-rate, and surface wind velocity is described by a Geophysical Model Function (GMF) [12]. It is desirable to continuously improve GMFs to be able to more precisely estimate the ocean surface wind velocity.

GMFs are based on measurements made from airborne as well as spaceborne scatterometers. Covering 90% of the ice-free ocean daily [9], satellite-based scatterometers provide a vast coverage of the earth as they orbit (Figure 1.1), but lack the spatial resolution desired to observe the inner core of tropical cyclones. With a range resolution between 2 and 10 km [9] satelite-based scatterometers are inefficient at measuring wind fields within TCs.

Figure 1.2. Department of Commerce WP-3D Orion Hurricane Hunter NOAA-42

To more accurately observe TCs, a locally deployed scatterometer with higher resolution is needed. Airborne scatterometers operate at lower altitudes (1-3 km) with finer resolution, and can focus in on specific regions of a storm by altering their flight plan. The University of Massachusetts at Amherst developed and maintains one such airborne scatterometer, the Imaging Wind and Rain Airborne Profiler (IWRAP) [4].

IWRAP was designed and built by the UMASS Microwave Remote Sensing Laboratory (MIRSL). It is seasonally deployed aboard one of two National Oceanic and Atmospheric Administration (NOAA) WP-3D Orion "Hurricane Hunter" aircraft (see Figure 1.2) based out of MacDill AFB in Tampa, Florida. IWRAP is a dual-frequency (Ku- and C-band), conically scanning, dual-polarized scatterometer capable of deriving ocean surface wind vectors as well as atmospheric wind fields [4]. Data gathered by IWRAP allows scientists to improve aforementioned GMFs.

For hurricane season 2008 the sensitivity of the IWRAP scatterometer was increased by increasing average transmit power through pulse compression. A new control system was also implemented which allows for more flexibility with respect to radar parameters when running the IWRAP radar system.

This thesis outlines the improvements made to the IWRAP system for hurricane season 2008. It explains the process of implementing a pulse compression scheme and redesigning the control system, along with all hardware and software modifications that were necessary to accomplish these upgrades. This thesis also explains the implementation of an optimal "hybrid" transmit waveform used during the 2008 hurricane season. Laboratory and field test data demonstrate its performance.

CHAPTER 2

IWRAP OVERVIEW

2.1 Doppler Radar and Scatterometry

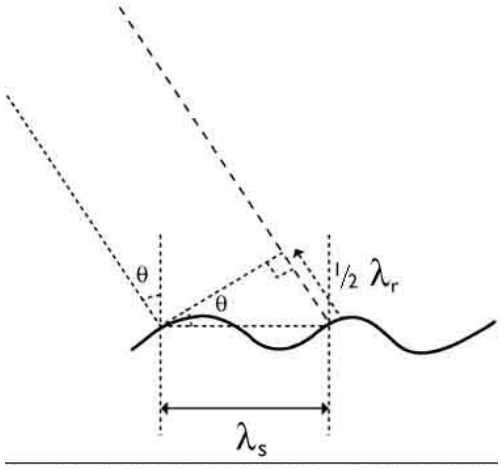

Figure 2.1. Diagram of Bragg scattering where λ_s is the sea surface wavelength, λ_r is the radar wavelength, and θ is the incidence angle

The first spaceborne scatterometer flew as part of the Skylab missions in 1973 and 1974, demonstrating that spaceborne scatterometers were indeed feasible [6]. Since then, various spaceborne scatterometers have been used to make measurements of wind velocity from space. Presently, the Advanced Scatterometer (ASCAT) and SeaWinds are the two operating spaceborne scatterometers. ASCAT is a C-band scatterometer aboard the European Space Agency's (ESA) Meteorological Operational (MetOp) platform. It collects data from three fan-beam antennas with different look angles (from 25-65^o) to retrieve a wind vector [7]. ASCAT uses a frequency-modulated transmit signal. SeaWinds is a Ku-band scatterometer built by the Jet Propulsion

Laboratory (JPL) aboard NASA's QuikSCAT satelite. SeaWinds employs a single 1-meter parabolic antenna dish with twin offset feeds for vertical and horizontal polarization. The antenna spins at 18 rpm, scanning two pencil-beams at incidence angles of 46^0 (H-polarization) and 54^o (V-polarization). This system uses a pulse-modulated transmit signal. Both instruments have a nominal spatial resolution of 50 km on the Earth surface. While the primary use of scatterometers is to measure near-surface winds over the ocean, scatterometer data are also being applied to the study of vegetation, oil production, soil moisture, polar ice, and global weather change.

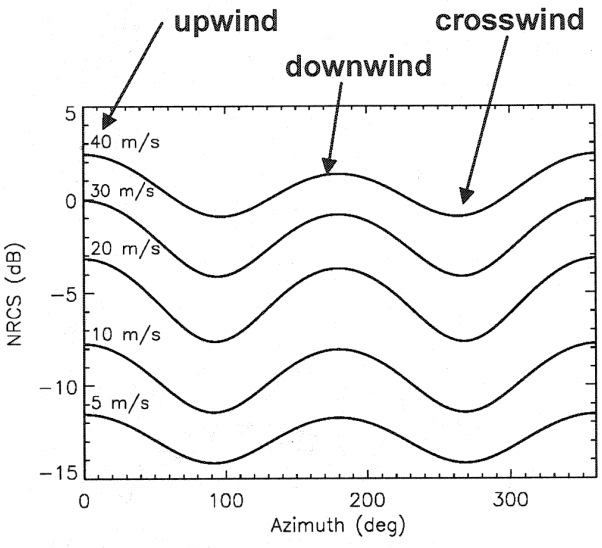

Figure 2.2. NRCS response versus the relative wind direction at different wind speeds at 30^o incidence and VV polarization [8]

The fact that wave size is governed by local wind speed [5] allows airborne scatterometers to estimate near surface ocean wind vectors by measuring the Bragg scattering from wind induced waves. For this reason, and through the use of GMFs, wind speed can be estimated by measuring the NRCS of the ocean surface. Figure 2.1 shows how the radar signal reflects off waves with respect to wavelength and incidence angle, while

$$\lambda_s = \frac{\lambda_r}{2sin(\theta)}$$

gives the mathematical relation between ocean wavelength (λ_s), radar wavelength (λ_r), and incidence angle (θ) defined for Bragg resonance. The NRCS of the ocean surface depends on azimuth angle relative to the direction of wave propogation. As shown in Figure 2.2, the NRCS is lowest when looking crosswind (90^o and 270^o) and at its peak when looking upwind (0^o).

IWRAP is also a Doppler radar capable of measuring wind speeds inside tropical cyclones using raindrops as tracers. The returned radar signal reflected by the raindrops are compared in frequency to the transmit signal. The frequency shift, up or down, gives a radial velocity measurement as seen in the following equation:

$$\Delta f = \frac{2v_r}{\lambda}$$

where,

$$\begin{aligned} \Delta f &= \text{change in frequency (Hz)} \\ v_r &= \text{radial velocity (m/s)} \\ \lambda &= \text{wavelength (m)} \end{aligned}$$

2.2 IWRAP Geometry

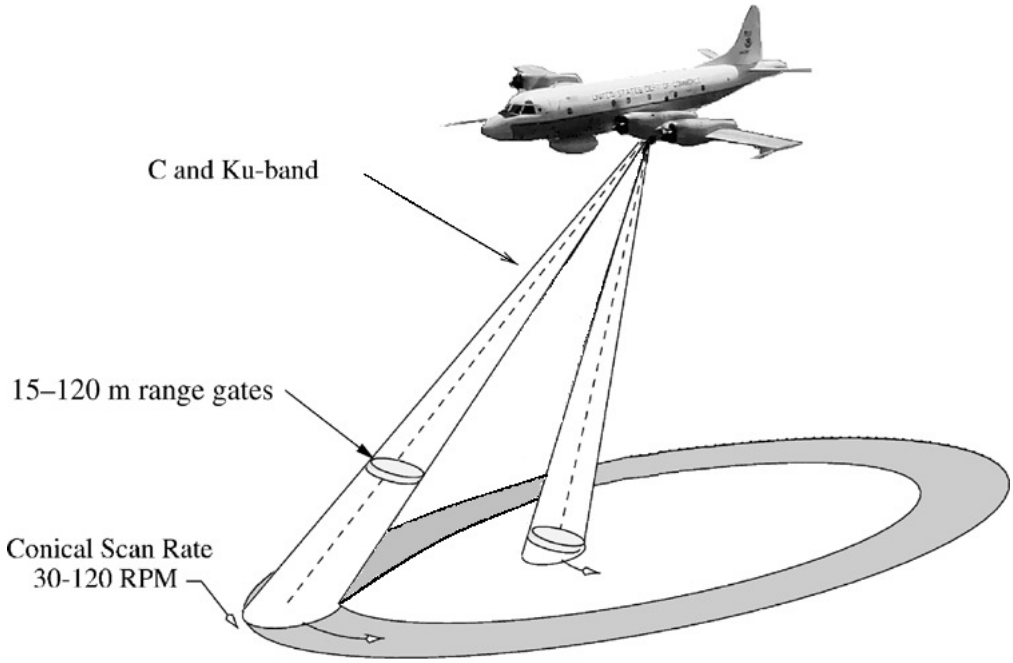

Figure 2.3. Diagram of IWRAP geometry

IWRAP conically scans the ocean surface with each antenna at 30-120 RPM as shown in Figure 2.3. Both antennas create pencil beams at incidence angles of approximately 30 and 50 degrees off nadir. Both C and Ku frequency bands produce two consecutive transmit signals within each PRI with center frequencies corresponding to the two scan angles. The typical case for the 2008 hurricane season was to use pulse compression at the larger angle to account for the increased atmospheric losses associated with the greater range. A simple pulsed transmit signal was then used at the smaller angle since there often exists sufficient average power to observe the ocean surface echo through rain. This is the basis for the Hybrid Transmit Waveform (HTW) introduced for the 2008 hurricane season, which will be explained in greater detail in Section 4.3.

2.3 IWRAP Specifications

While IWRAP has been operated with similar radar specifications for over a decade, parameters have changed slightly from year to year. The radar specifications used during hurricane season 2008 are shown in Table 2.1. Many of the values in this table are fixed, while the variable parameters are denoted with a (∗). It is possible to change these variables at any point during a reconaissance mission, yet many of them remained unchanged throughout the 2008 season. This includes the scan rate of 60 RPM and pulse-width of 200 ns. The deployment altitude depended on the flight for various reasons, and picking a viable PRF depended on the altitude of the flight because of limitations with respect to unambiguous range.

IWRAP Specifications

Parameters	**C-band**	**Ku-band**
Incidence angles (deg)	30, 50	30.1, 48.6
Tx Frequency (GHz)	5.42, 5.015	13.92, 12.87
∗ Flight altitude (m)	1500 - 5000	1500 - 5000
Tx Power Peak (dBm)	42	42
∗ Pulse-width (ns)	200	200
∗ Chirp-width (μs)	10	10
∗ Chirp bandwidth (MHz)	2 or 4	2 or 4
∗ PRF (kHz)	15	15
Azimuth (deg)	0 - 360	0 - 360
∗ Scan Rate (RPM)	60	60
	Dual-pol Antenna	**Single-pol Antenna**
Gain (dBi)	20, 21.6	28.8 - 25.8
E-plane HPBW (deg)	5.2, 10.2 (az)	5, 8.1 (el)
H-plane HPBW (deg)	26, 10.9 (el)	8, 6 (az)
Polarization	HH	VV

Table 2.1. C- and Ku-band IWRAP system specifications for the 2008 hurricane season. All parameters denoted with an (∗) are typical values as they are user defined. Note that for C-band the H-polarized side of a dual-polarized antenna was used, while for Ku-band a single-polarized (vertical) antenna was used.

2.4 System Description

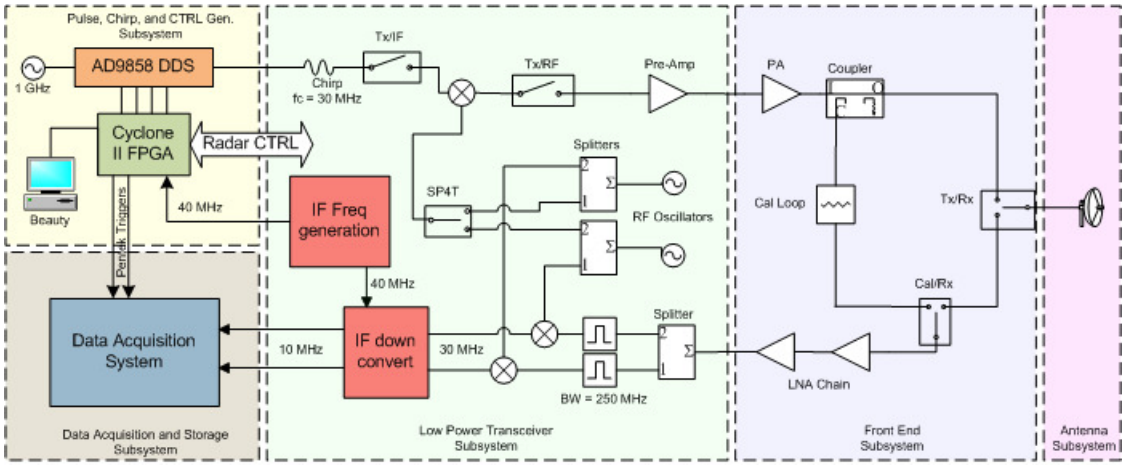

Figure 2.4. Block-diagram of basic radar subsystems. (Note: This diagram shows the basic radar design. Ku- and C-band both have similar designs as shown here, but Figures 2.5, 2.6, and 2.9 show actual Ku- and C-band transciever, and control subsystem schematics.)

Figure 2.4 shows a basic block diagram of the entirety of one IWRAP radar system (both C- and Ku-band radar systems are similar, but not identical), while the following section explains either transceiver subsystem. Although much work was done to improve IWRAP for the 2008 hurricane season, the transceiver and antenna subsytems as well as both Ku- and C-band front-ends remained basically unchanged. The following sections explain the IWRAP radar system after all upgrades were completed for the 2008 hurricane season. The chapters that follow explain how each subsystem was improved over their previous design. All improvements were made either to help implement pulse compression, or to make the system more reliable and user friendly.

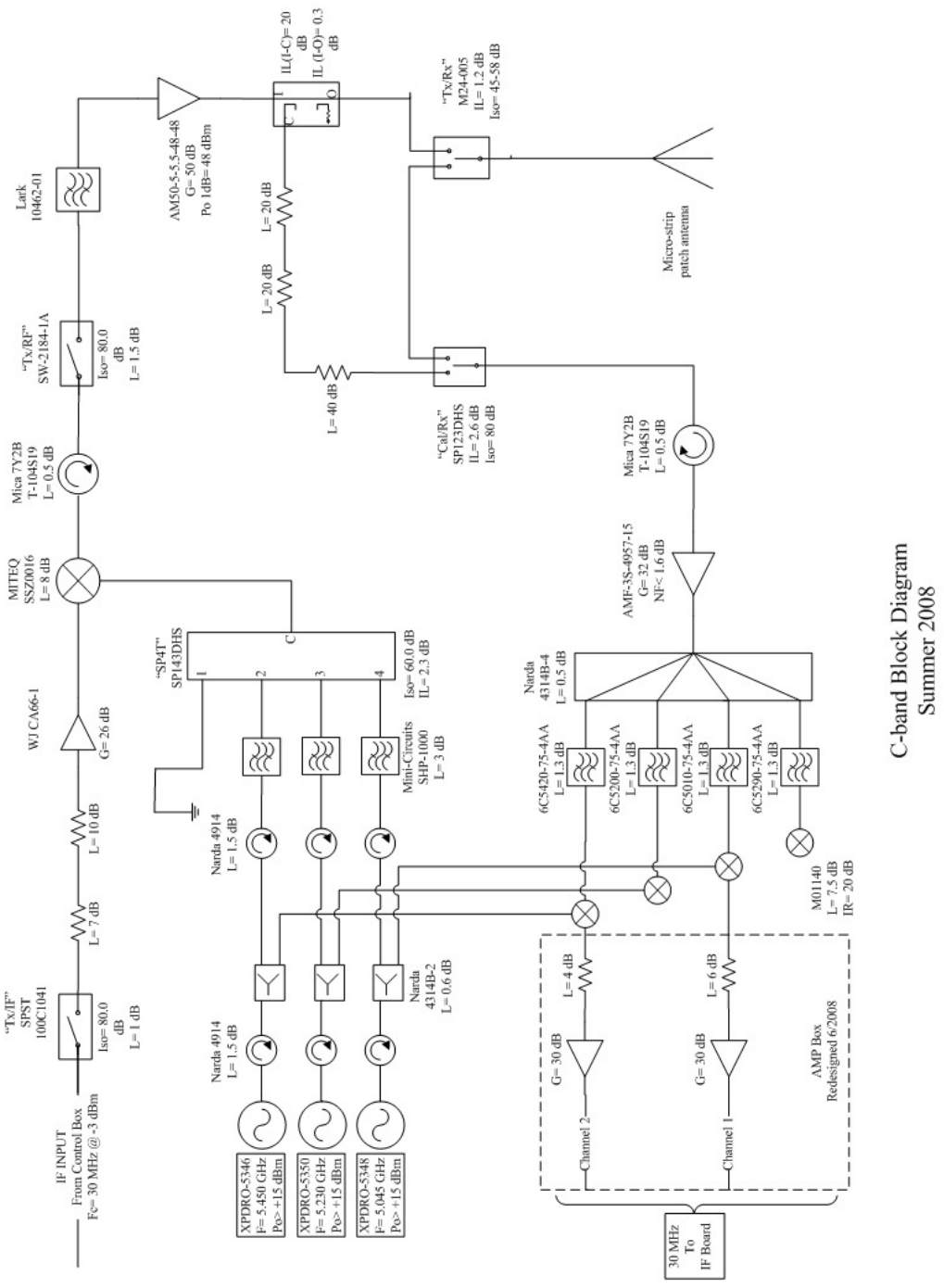

Figure 2.5. Block-diagram of IWRAP C-band sub-systems for hurricane season 2008

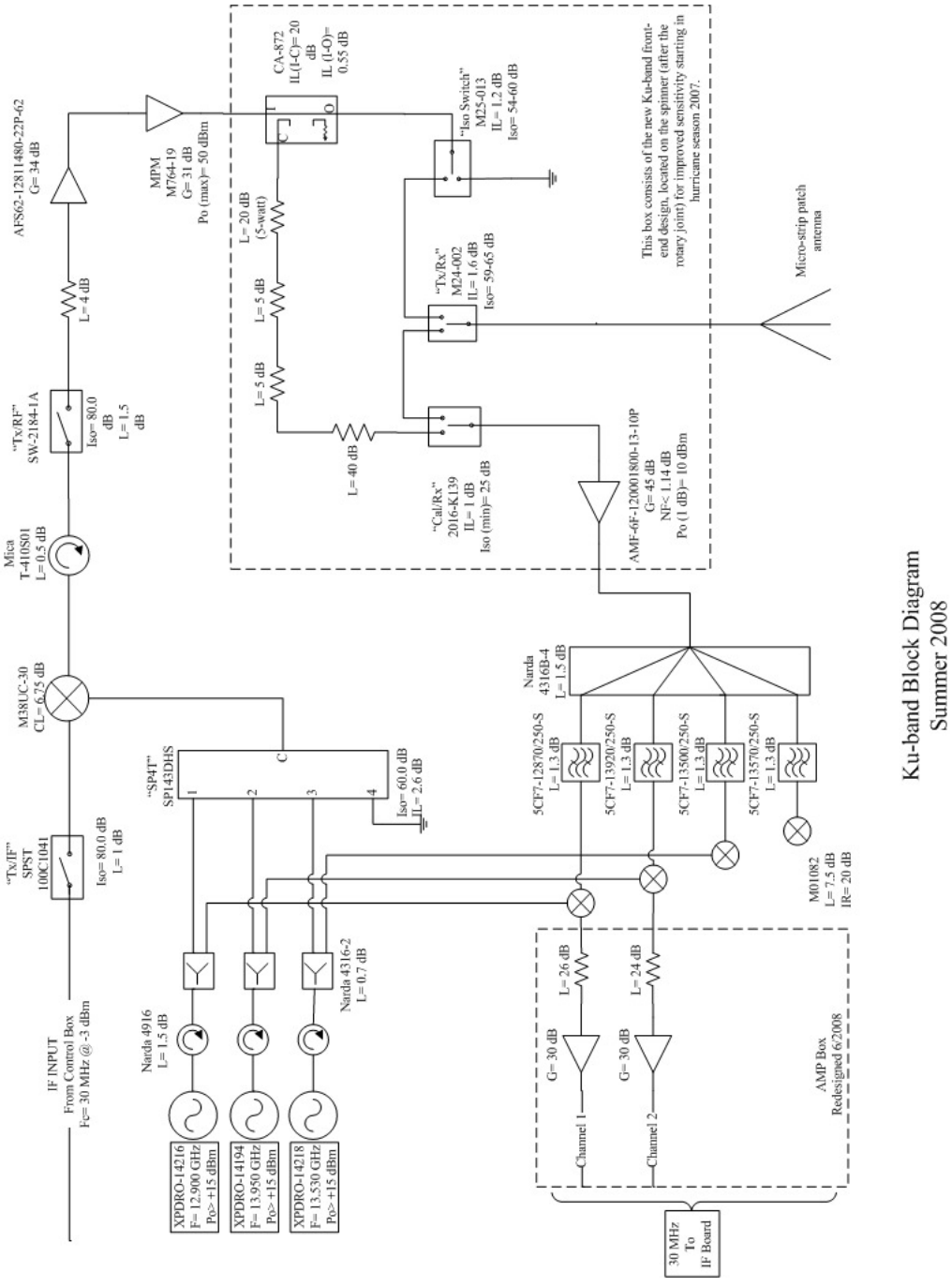

Figure 2.6. Block-diagram of IWRAP Ku-band sub-systems for hurricane season 2008

2.4.1 Transceiver and Front-End

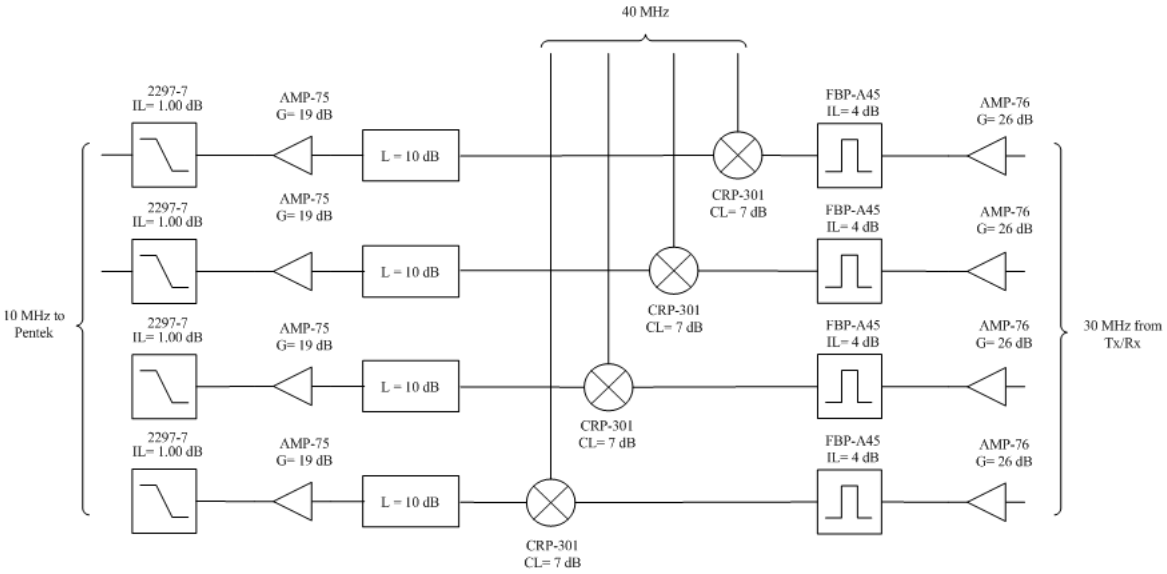

Figure 2.7. IF board, used for down-conversion of 30 MHz signal to 10 MHz

In the transceiver subsystem the IF transmit signal is mixed with two RF sources creating two consecutive signals. At Ku-band two oven controlled oscillators operating at 12.9 and 13.95 GHz are used as the frequency sources, while C-band utilizes frequencies of 5.045 and 5.45 GHz, respectively (the C- and Ku-band microstrip patch antennas were designed to steer these frequencies accordingly). After upconversion to radio frequency, both signals pass through a pre-amplifier, and then to a high-power amplifier before reaching the front-end. In the front-end the signals pass through a 20 dB coupler. The coupled output is sent to the receiver through a calibration loop, while the through port is sent to the antenna. A high-power switch before the antenna controls whether the radar is in transmit or receive mode. The received signal is amplified by a low noise amplifier and is then split to be mixed down to intermediate frequency (IF) by the appropriate RF signals used for up-conversion. These two IF signals are again down-converted (to 10 MHz) and sent to the data acquisition sub-

system. Data packets containing UTC time stamp, location, navigation, and antenna position are stored in high-capacity RAIDS for post-processing [3].

Diagrams of the IWRAP transceiver and front-end for both C- and Ku-band subsystems are shown in Figures 2.5 and 2.6. A diagram of the IF board used to downconvert the 30 MHz signal to 10 MHz is shown in Figure 2.7.

2.4.2 Radar Timing and Control Subsystems

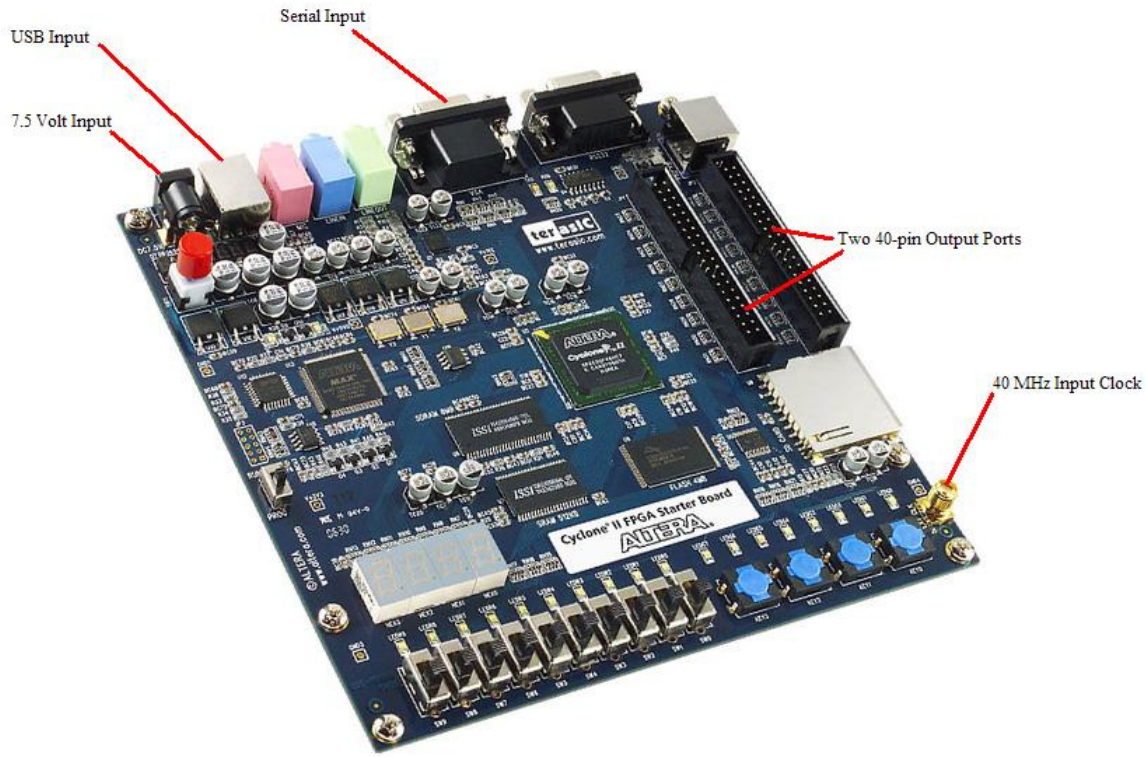

Figure 2.8. Altera Cyclone II FPGA Development Kit (photo courtesy of Altera)

In previous hurricane seasons an outdated radar timing and control system had been used, which did not allow for the flexibility needed to implement pulse compression or a HTW. For this reason, a new control system was developed for the 2008 hurricane season. The new control system consists of an Altera Cyclone II Field-

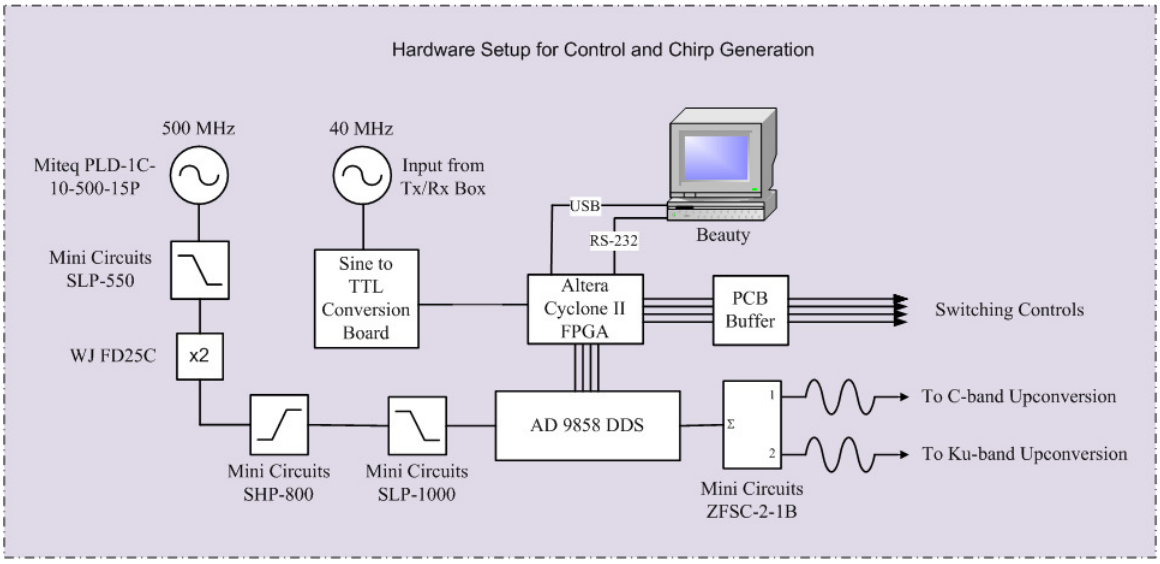

Figure 2.9. Block-diagram of the FPGA and DDS I/O

Programmable Gate Array (FPGA) Development Kit and a buffer board designed to convert the low-voltage TTL outputs of the FPGA to the 5V TTL required by the various radar switches and digital receiver.

The FPGA is programmed and controlled by a new host computer (Beauty), which replaces the old computer (Beast). Using Quartus software (included in the FPGA development kit) and a 40 MHz reference clock input, a timing design was created to produce all signals and triggers needed to control the radar system. Also generated by the FPGA are the waveforms needed to program the Direct Digital Synthesizer (DDS). The FPGA board is shown in Figure 2.8, while Figure 2.9 shows a block diagram of the FPGA and DDS setup. A more thorough description how the FPGA design executes is provided in Chapter 3. The Quartus design files are explained in Appendix A.

To improve the user-radar interface a new Graphical User Interface (GUI) was developed to help run the new IWRAP control and data collection systems. It also generates a real-time display, showing a basic plot of received power and encoder

values. The GUI takes user inputs including pulse-length, chirp bandwidth, and pulse-repetition frequency (PRF), and forwards them to a C-program that controls the FPGA over an RS-232 serial cable. The GUI makes it possible to run the entire IWRAP system from one station, making the system as a whole more efficient and easier to operate.

2.4.3 Pulse/Chirp Generation

In previous hurricane seasons a simple 30 MHz IF oscillator created the baseband IF signal. This was sufficient for a pulsed transmit waveform, but the addition of pulse compression introduced the need for a more complicated transmit waveform. Thus, a DDS was integrated into the pulse/chirp generation subsystem. The DDS now creates the IF signal, which is either a 30 MHz single tone or a linear frequency-modulated 'chirp' centered at 30 MHz. An Analog Devices AD9858/PCBZ DDS was chosen for this application for its frequency sweeping capabilites, as well as its ability to store multiple profiles. The DDS is controlled by the FPGA, and requires an input reference clock of 1 GHz. This DDS can store up to four different profiles enabling rapid (within 100 ns) switching between user-defined outputs, in this case either a pulse or a chirp. The programming of the DDS is explained in Section 4.3.1.

2.4.4 Antennas

While IWRAP had previously been configured to be able to collect dual-polarization data, for the 2008 hurricane season single-polarization data was collected at both frequency bands. At Ku-band, a single-polarized (vertical) antenna was used, while at C-band the h-polarized half of a dual-polarized antenna was used. As opposed to previous hurricane seasons, the polarization did not change for either C- or Ku-band the entire season. The antennas used are shown in Figures 2.10 and 2.11.

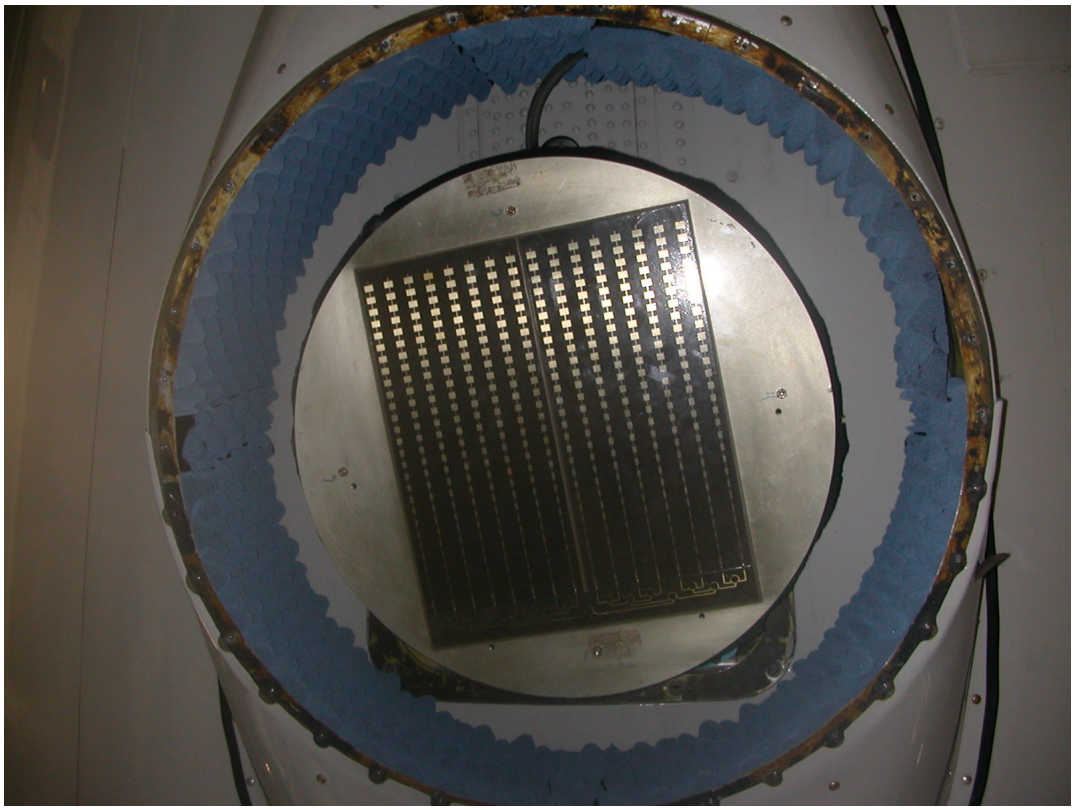

Figure 2.10. Mounted Ku-band single-polarization (vertical) antenna used for the 2008 hurricane season

Figure 2.11. C-band dual-polarization antenna used for the 2008 hurricane season (only H-polarization was used)

2.4.5 Data Acquisition System and Storage

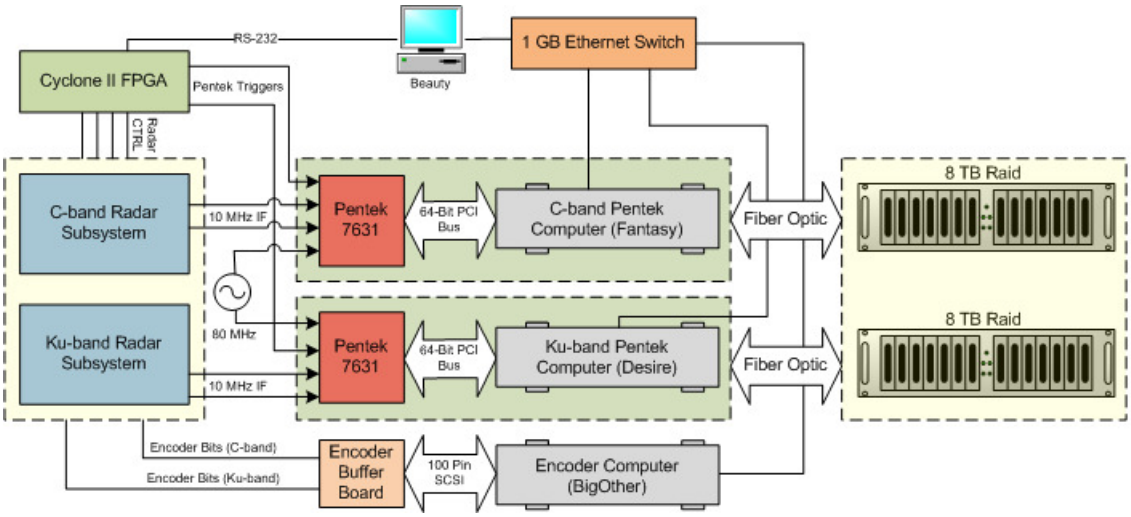

Figure 2.12. Block-diagram of data subsystems

A block diagram of the IWRAP data acquisition system used for hurricane season 2008 is shown in Figure 2.12 and consists of the following components:

1. Two data acquisition computers (Fantasy and Desire), each housing a Pentek 7631 digital receiver.

2. One computer (BigOther) housing a digital I/O card for reading encoder signals

3. One host computer, used to control the radar and view the real-time display (Beauty).

4. Two 8 TB Redundant Arrays of Independent Disks (RAIDs) (four RAIDs were used for the 2008 hurricane season but room exists for just two at one time on the aircraft).

5. Two encoders (one located on each spinner) and a PCB designed to buffer all encoder values.

Each Pentek card takes an input clock of 80 MHz, two 10 MHz IF channels from the radary subsystems, and a trigger. The data acquisition computers perform final receiver down-conversion, demodulate I and Q data, store all raw data on 8 TB RAIDs, and broadcast the data as UDP packets overa gigabit ethernet link. BigOther stores the encoder data (received from the encoder buffer board over a 100-pin SCSI connector), which is a numerical value associated with the azimuthal position of each antenna. This data is appended to the raw data files for use in post-processing.

For hurricane season 2008 the IWRAP data acquisition system was improved over previous seasons. With the added processing power of the host computer (Beauty), a new real-time display was designed. The new real-time display takes raw data broadcast from the data acquisition computers and processes and plots it versus range for both channels on each the C- and Ku-band radar systems. Also plotted on the real-time display are the encoder values for both radar systems. This display helps the user easily determine if all radar subsystems are working properly. The design of the real-time display is explained further in Section 3.4.

2.4.6 IWRAP Components: Aircraft Layout

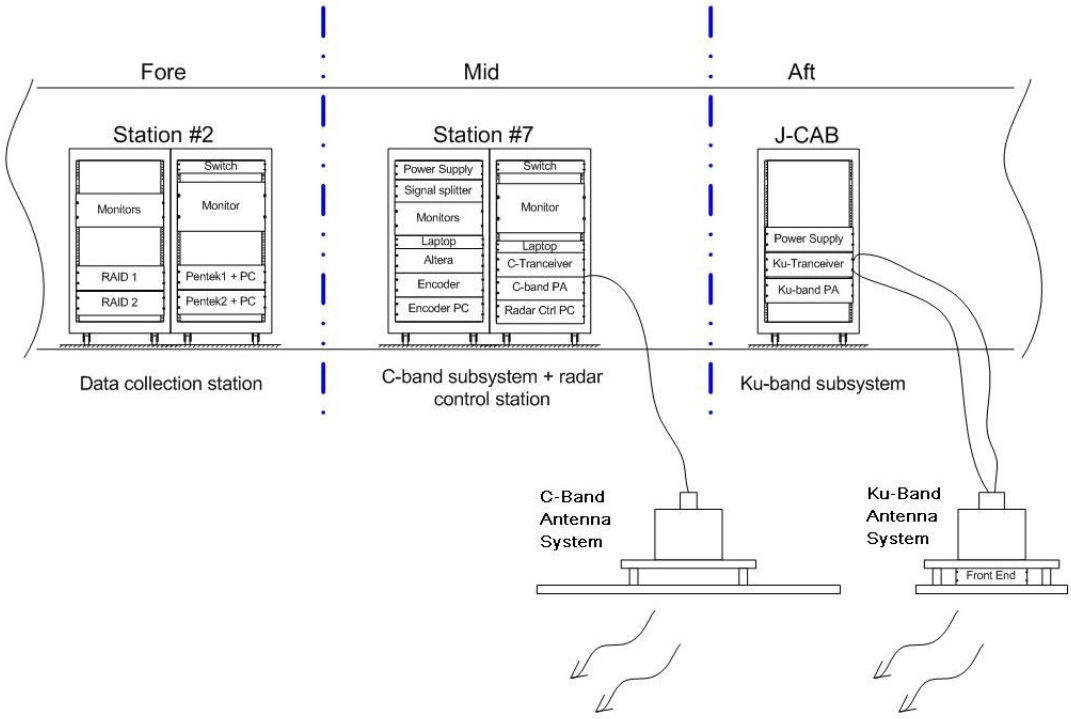

Figure 2.13. Diagram of IWRAP radar component locations on NOAA-42 (diagram courtesy of Tao Chu). Note the Ku-Band front-end located on the antenna

A diagram showing the locations of the IWRAP components is shown in Figure 2.13. The various IWRAP components are located in three stations throughout the aircraft. Station 2 is located toward the front of the aircraft, and houses the data acquisition computers as well as the RAIDs. Station 7 is located in the center of the aircraft, and houses the majority of the radar components. This is the station from which the radar is controlled, and the real-time display is viewed. Station 7 also houses the C-band transceiver, amplifier, and power supply, as well as BigOther and Beauty. Towards the rear of the aircraft located in a rack named the "J-cab" are the Ku-band transceiver, power supply, and high-power amplifier. The Ku-band front-end, which was moved for hurricane season 2007, is located on the Ku antenna.

The locations of both C- and Ku-band antennas with respect to the aircraft can be seen in Figure 2.14.

Figure 2.14. Location of C- and Ku-band scatterometers on N42

CHAPTER 3

IWRAP CONTROL SYSTEM

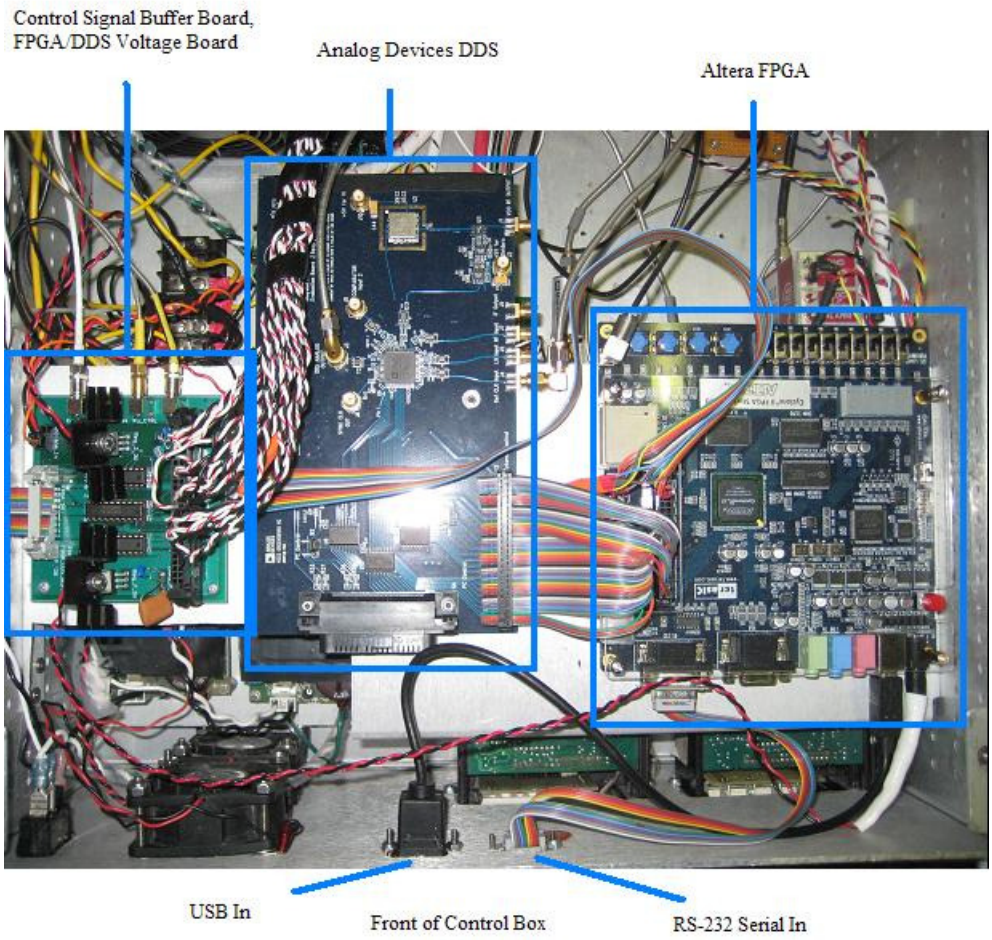

Figure 3.1. FPGA, DDS, and PCB buffer board mounted in the control box

The new IWRAP control system consists of an Altera Cyclone II FPGA Development Kit, a new GUI with various user inputs, control system software which interfaces the GUI and the FPGA, and a PCB which pulls up and buffers the radar

control signals and Pentek triggers. The new control system was essential in implementing pulse compression in the IWRAP system, and also increases the number of user-defined parameters allowing the user to tailor the system depending on deployment scenario and desired transmit/receive mode. A picture of the FPGA, DDS, and control signal buffer PCB mounted in the control box is shown in Figure 3.1.

3.1 FPGA Design and Control Software

The newly created FPGA software takes inputs from the GUI and calculates wait-states, which correspond to pulse-widths, delays, and triggers. Figure 3.2 shows the wait-states for the FPGA control system, and lists what each wait-state pertains to.

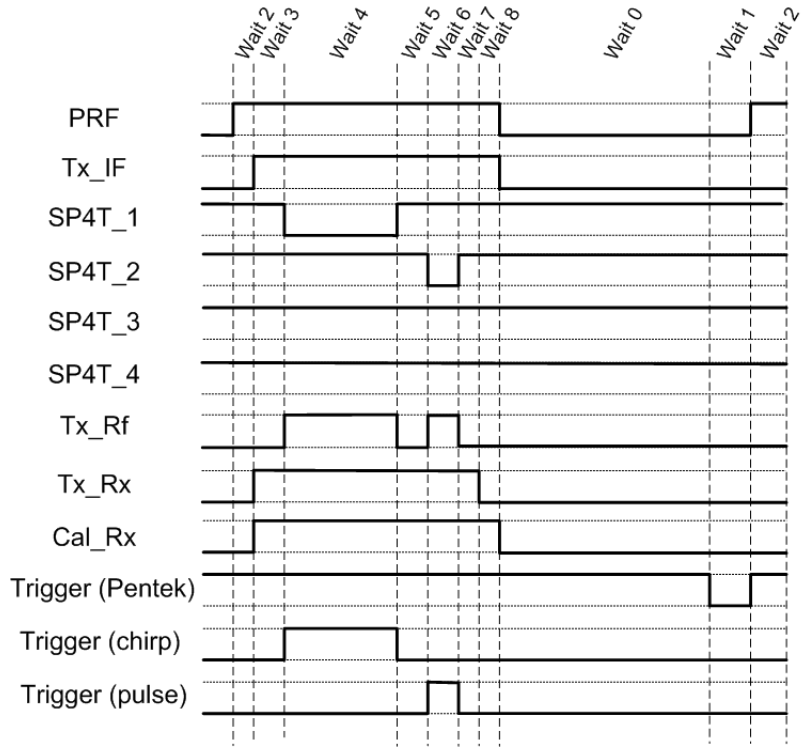

Figure 3.2. Wait-states used for IWRAP timing and control signals for one PRI (not drawn to scale). The location of each switch pertaining to these control signals can be located in Figures 2.5 and 2.6. A description of each wait-state is given in Table 3.1.

Wait-State	Wait-State Function
Wait 0	Receive Time
Wait 1	Pentek Gate Toggle
Wait 2	High-power Switch Delay (1)
Wait 3	High-power Switch Delay (2)
Wait 4	Chirp-width
Wait 5	Time between chirp and pulse
Wait 6	Pulse-width
Wait 7	High-power Switch Delay (3)
Wait 8	High-power Switch Delay (4)

Table 3.1. List of the nine wait-states and their functions

The Cyclone II FPGA development kit comes with an Altera EP2C20F484C7 device, and was chosen for its dual 40-pin outputs and user-friendly development software (Quartus II Version 7.0). The inputs and outputs used were shown earlier in Figure 2.8. The FPGA design is created in a Quartus project file, and is composed of 5 blocks consisting of .v (verilog) and .tdf (test design file) files. Once compiled, these design files create Quartus block/schematic files used in the final Quartus block/schematic design shown in Figure 3.3.

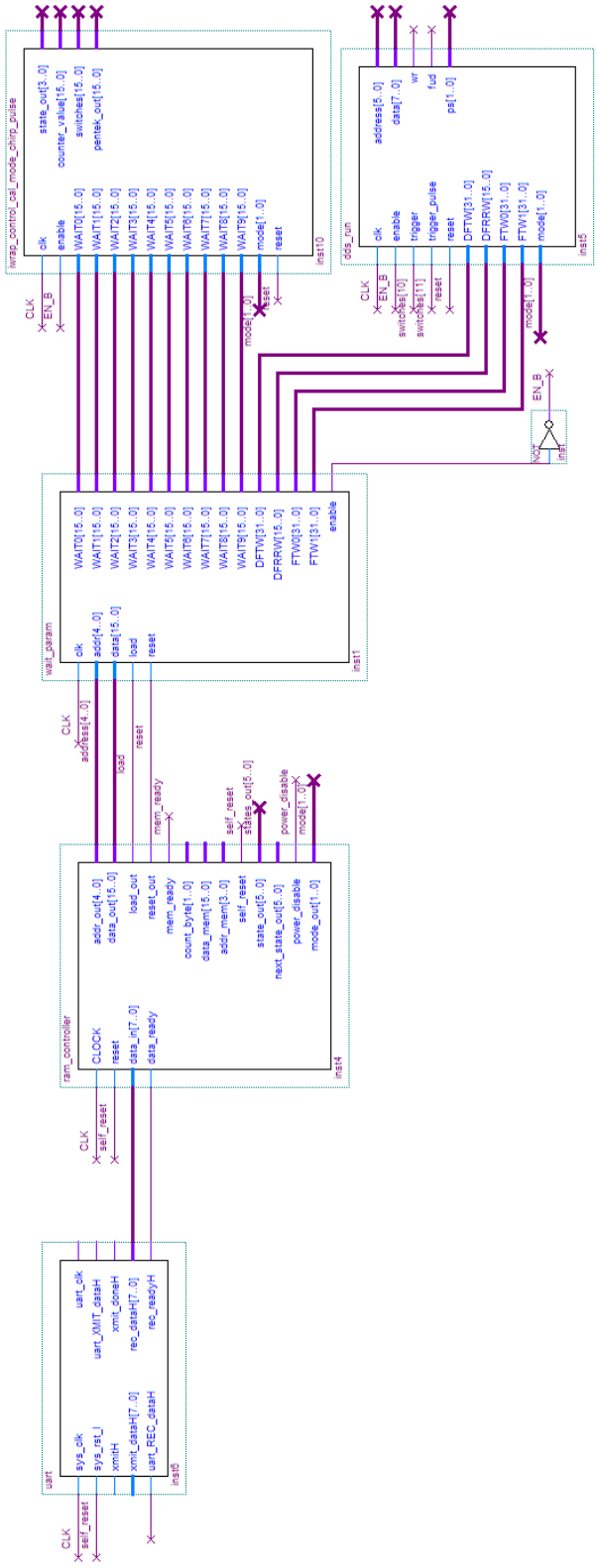

Figure 3.3. FPGA Quartus block/schematic

The FPGA Quartus block/schematic employs an RS-232 serial input from a C-program on Beauty, which sends data to be divided by the UART block into 8-bit packets. These packets are passed through each block, and eventually create the output control signals, DDS inputs, timing delays, and triggers needed to run the radar. The inputs, outputs, and code used to create the Quartus block/schematic design are described in Appendix A.

3.1.1 Control Software: start-iwrap

The FPGA requires a serial input over an RS-232 cable to input data into the Quartus block/schematic design. A C-program named 'start-iwrap' pulls data from the IWRAP GUI, and sends it to the FPGA (the GUI will be explained in Section 3.3). The start-iwrap C-program was derived from the program 'sonic', developed by MIRSL director Stephen Frasier, and the program 'trial-c-code' used in the UMASS Marine Radar. It was altered by MIRSL student Albert Genis in October of 2007, and adapted for this IWRAP application in the Spring of 2008 with the help of MIRSL and JPL employee Dragana Perkovic.

The 'start-iwrap' C-program is explained in the following list, in the order in which it executes.

- Define variables. The C-program 'start-iwrap' first defines all variables. These variables include all user-defined variables seen on the GUI as well as data/time information.

- Open parameter file. The parameter file is opened and the parameters are read into the program. The parameter file is then closed.

- Copy parameter values to variables, and adapt the units. Once the variables (mode, pulse-width, chirp-width, time between pulses, prf, chirp bandwidth, DDS data, etc.) are copied, the units are adapted from the values entered into

the GUI to the value needed to correctly calculate timing and mode values. The high-power switch delays are hard-coded here, as are the DDS center frequency (30 MHz), DDS clock (1 GHz), and FPGA clock (40 MHz).

- Calculate the eight wait-states and DDS values. The next part of the code adapts the timing scheme from a value of time in seconds, to a number of clock cycles. As an example, for a pulse-width of 200 ns, and using the FPGA clock of 40 MHz, the FPGA code will count 8 clock cycles for wait-state 6 (refer to Figure 3.2):

$$N(8) = \frac{PW(200ns)}{T(25ns)}$$

where N is the number of clock cycles, PW is the pulse-width, and T is the period of the FPGA clock. This is done for all delays as well as DDS registers, which are calculated in a slightly different way and will be further explained in Appendix B.

- Open serial port and write values. This part of the code is where the values that intially were input by the user into the GUI are sent to the FPGA via the RS-232 serial port. Each wait-state is comprised of 16-bits (some DDS values are 32-bits, some are 8-bits) divided into 8 bit packets. The FPGA program was designed to take the 8-bit packets in the order defined in this part of the code to properly create the wait-states and DDS register values. At the end of this process the code indicates the end of writing to the FPGA, and the serial port is closed.

3.2 Control Signal Printed Circuit Board (PCB)

In order for the switching controls output by the FPGA to work with the IWRAP switches and Pentek triggers, the signals needed to be pulled-up from low-voltage

TTL (3.3 volts) to 5 volts. They also needed to be split as the FPGA creates only one signal for each switch, and with both radar systems running simultaneously there exists a need for two of each signal. Signal splitting is done before the signal is buffered as to not limit the current each signal delivers to its respective load. This buffer board also houses the voltage regulators used to create supply voltages for the DDS and FPGA. The FPGA requires an input voltage of 7.5 volts, so a 15 volt to 7.5 volt regulator is used. The DDS requires 3.3 volts, so a 5 volt to 3.3 volt regulator is used. Each regulator requires a heat-sink as the expended voltage creates substantial heat.

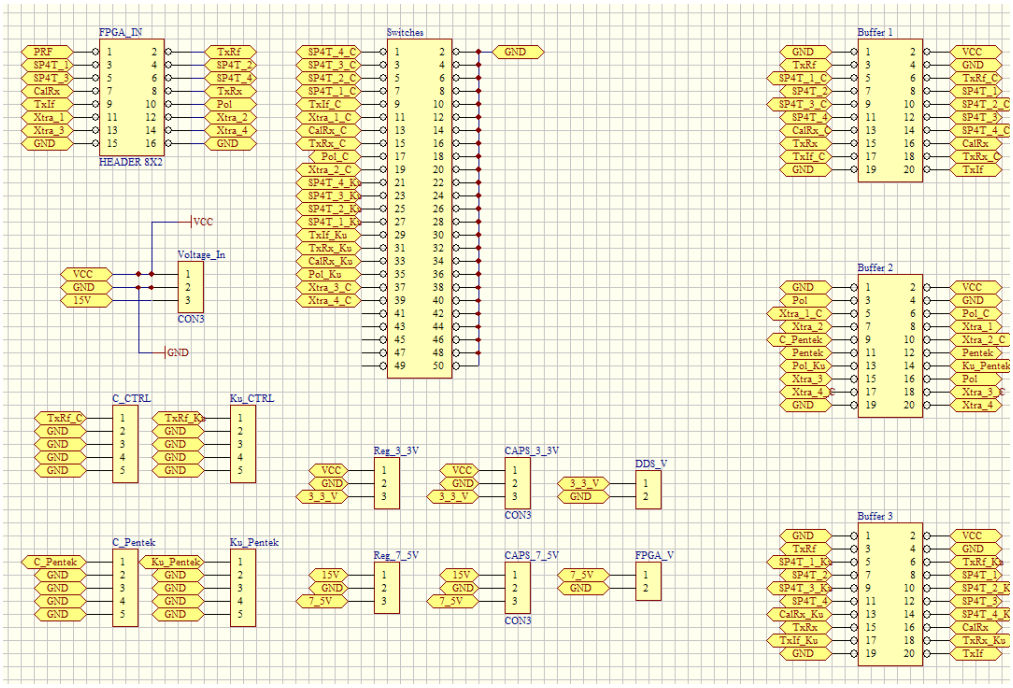

Figure 3.4. IWRAP FPGA control signal PCB buffer board: schematic designed in Protel99

These functions were accomplished by creating a PCB which houses three pull-up buffer chips, takes the FPGA signals as an input, and outputs the signals via a 50-pin header connector. For buffer chips, the STMicroelectronics 74ACT244B chip was chosen for its high-speed buffering (typically 4.6 ns) and because it can pull-up

the voltage of its input signal to a VCC of up to 5.5 volts. A design of the PCB was created using Protel99 software. To do this a schematic of all signals and connections is created, as seen in Figure 3.4. Next a layout of each component that will be used on the PCB is created, with exact dimensions for each socket. These chip/header layouts are then placed in a physical PCB layout, which is the actual layout the PCB will have when created. Using the Protel99 software, the PCB layout routes all connections. Finally layers of ground planes, silk screening, and solder masks (which can be seen in Figure 3.5) are added. Once this design is created the software creates design files, which are sent to AdvancedCircuits (www.4pcb.com) who create the physical PCB. The finished PCB located in the IWRAP control box can be seen on the left of Figure 3.1.

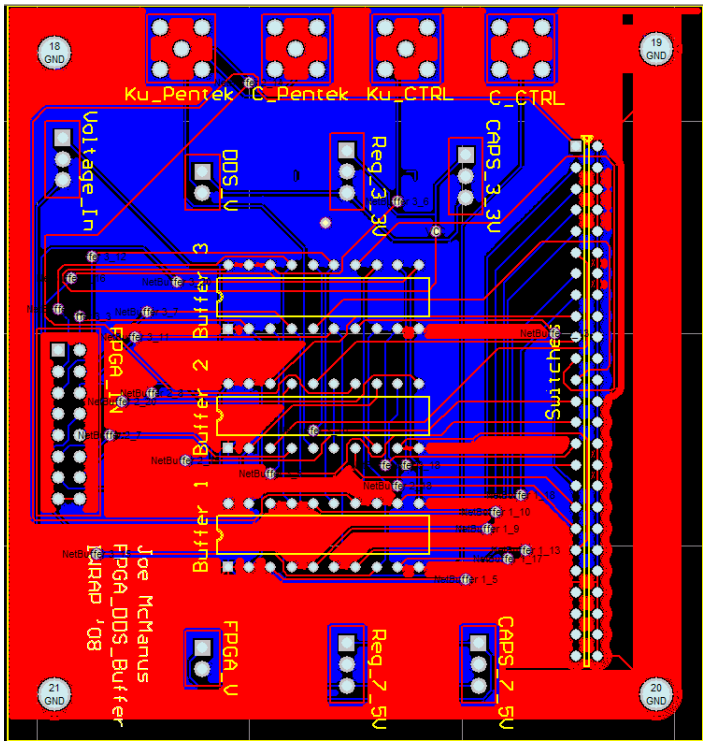

Figure 3.5. IWRAP FPGA control signal PCB buffer board: physical layout designed in Protel99

3.3 GUI

Adding many new user defined variables to the IWRAP system created a need for a more organized radar control interface for IWRAP users. For this reason, and to make IWRAP easier to operate, a new Graphical User Interface (GUI) was developed by Stephen Frasier. The program 'igui-create' creates the GUI by simply typing 'iwrap' on a command line when logged into the Beauty host computer, and allows the user to define all variables seen in the left-hand column of Figure 3.6.

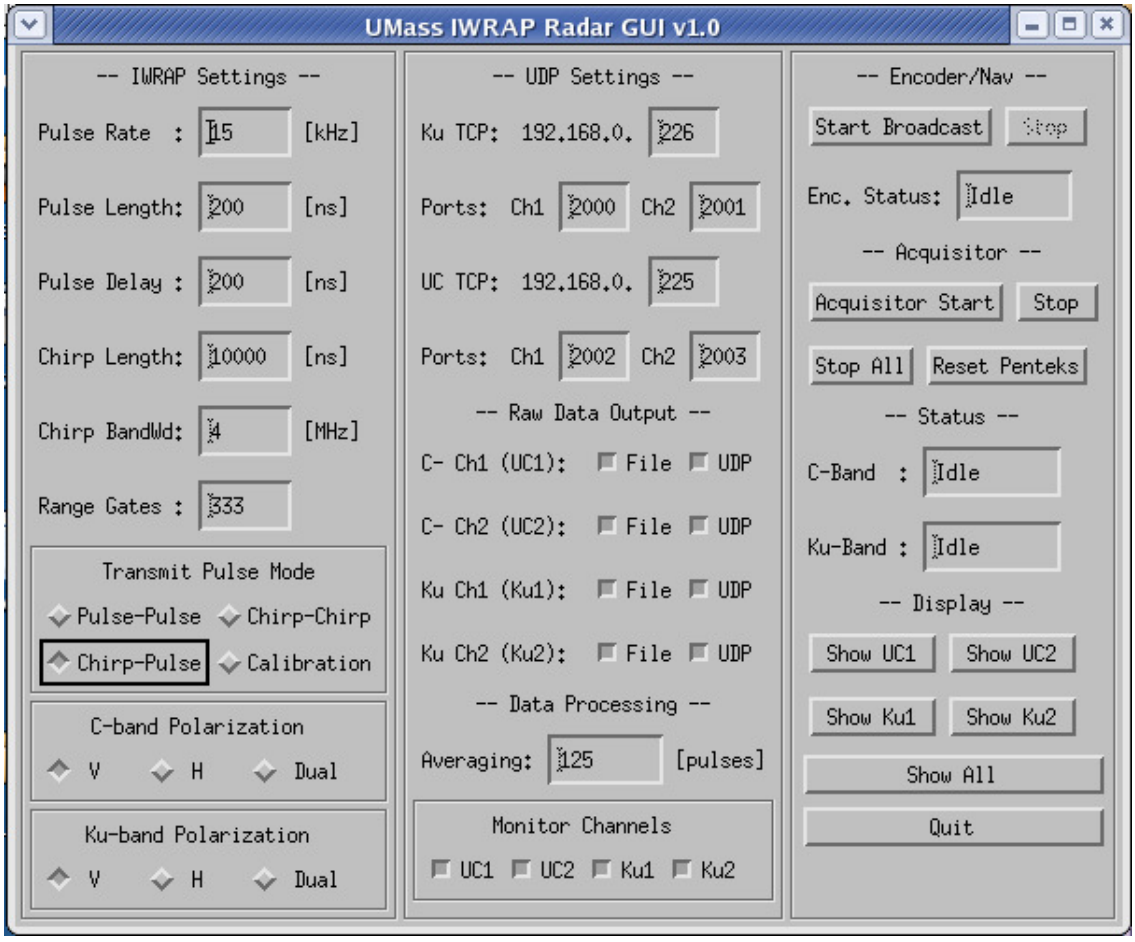

Figure 3.6. IWRAP Radar GUI v1.0. The radar parameters seen in this GUI are the settings primarily used for the majority of the reconnaissance missions for hurricane season 2008.

At the end of the the 'igui-create' program, control is handed over to the 'igui-event' program. While the 'igui-create' program creates all buttons and input windows for the GUI, 'igui-event' (created by Jeremy Vight) performs the actions of starting the encoders, starting the acquisitor, and sending information from the GUI to the correct configuration files. This program also creates the files where the collected data is saved. Appendix C explains the different sections of the new IWRAP GUI.

The new GUI is also beneficial when in search of an ideal pulse compression scheme to use for deployments. The flexibility of the improved system allows the operator to switch between different modes, bandwidths, and pulse-pair averaging very easily. Having the real-time display integrated into the GUI is a nice feature allowing the user to quickly assess system performance. The new GUI also proved to make IWRAP very user-friendly on deployments. It allowed IWRAP operators to instruct those unfamiliar with running the improved radar system how to run it within a matter of minutes. This was a nice feature to have as the length of the missions can be tiring. It also alleviated the need of having two MIRSL students on each deployment, allowing some flexibility with travel and scheduling around missions.

3.4 Real-Time Display

For hurricane season 2008 a new real-time display was implemented. This display takes pulse-pair processed data and displays received power levels and encoder position. The real-time display pops up in a window when the 'Show UC1, UC2...' or when the 'Show All' buttons are pressed on the IWRAP GUI. When a single channel display button is pressed the 'igui-event' program calls 'idispfile', which creates a plotting window and displays power, velocity, and phase plots versus range. The 'Show All' button displays plots of power level versus range for all four channels as well as both encoder values, and leaves out the velocity and phase plots. This display

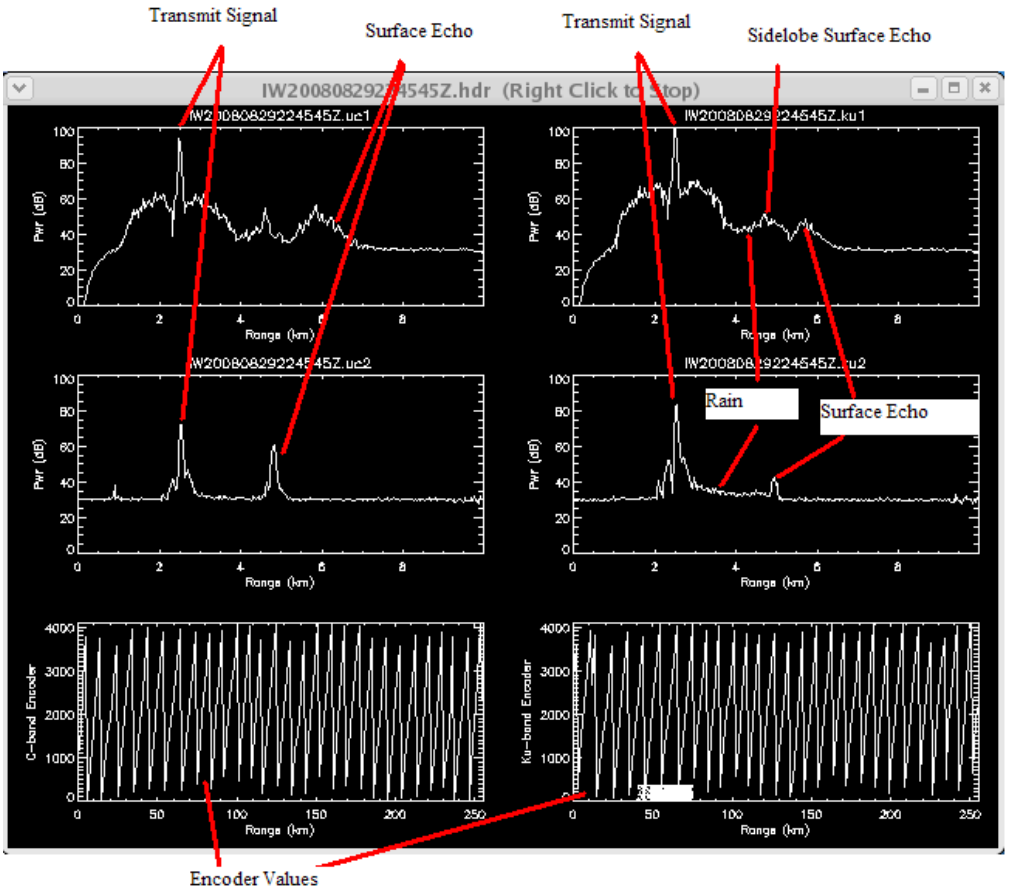

Figure 3.7. IWRAP real-time display. C-band is the left-hand column, Ku-band is on the right. The higher incidence angle which uses pulse compression (channel 1) is located above the lower incidence angle (channel 2).

runs until a network slowdown occurs, or if the user right-clicks or closes the window.

The real-time display created by Stephen Frasier is shown in Figure 3.7

CHAPTER 4

PULSE COMPRESSION

4.1 Introduction

IWRAP had previously been lacking sensitivity, especially at Ku-band. Because of the higher frequency the signal was greatly attenuated in high rain-rates. This problem was first addressed in 2007 when MIRSL student Tao Chu improved the senstivity of the system by locating the front-end of the Ku-band receiver closer to (on) the antenna, thereby reducing the Ku-band receiver noise figure. This helped, however more sensitivity was desired, so adding pulse compression to the IWRAP radar system was considered.

Pulse compression involves the transmission of a long coded pulse and the processing of the received echo to obtain a relatively narrow pulse. With this technique increased sensitivity is gained by transmitting larger average power, while the range-resolution capability of a narrow-pulse system is retained [13]. This method requires a modulated transmit waveform such as a Frequency Modulated (FM) 'chirp', and a more complicated receiver compared to pulsed radar systems.

Increasing the pulse-length increases the average transmit power of a radar system (as long as the PRF remains the same) while keeping the peak power relatively low. Keeping peak power low is important in the IWRAP airborne radar system as it is limited with respect to space and cost.

To show how pulse compression helps with respect to sensitivity, consider the radar range equation for meteorological applications:

$$P_r = \frac{\pi^3 P_t G^2 G_S \theta_1^2 c\tau |K|^2 Z}{2^{10}(\ln 2)\lambda^2 R^2 l^2 l_r}$$

where

P_t	=	peak transmit power (kW)
G	=	transmitting and receiving antenna gains
G_s	=	system gain between receiving antenna and receiver
λ	=	wavelength (m)
c	=	speed of light, 3×10^8 (m/s)
τ	=	chirp length (μsec)
θ	=	transmitting or receiving antenna 3 dB beamwidth
R	=	range to target (m)
l_r	=	finite receiver bandwidth loss (dB)
l	=	atmospheric loss (dB/km)
Z	=	reflectivity factor
B	=	chirp bandwidth

Here, $K = \frac{n^2-1}{n^2+1}$ where n is the complex refractive index of water. Solving for Z_{min} requires setting $P_r = P_n$, resulting in:

$$Z_{min} = \frac{2^{10}(\ln 2)\lambda^2 R^2 l^2 l_r P_n}{\pi^3 P_t G^2 G_S \theta_1^2 c|K|^2}$$

Z_{min} is the minimum signal the radar system can detect [3]. Having R^2 and λ^2 in the numerator, as well as P_t in the denominator of the equation for Z_{min} shows that the minimum detectable signal is limited by the altitude at which the system is deployed as well as the frequency and transmit power of the radar. These equations show that the smaller wavelength at Ku-band offers increased sensitivity compared to C-band, but the higher frequency also induces greater atmospheric attenuation and scattering thus lowering overall received power. For this reason SNR is more of a concern at the higher frequency.

An important figure of merit when considering a pulse compression radar system is the compression gain ($B\tau$), where B is the transmit chirp bandwidth and τ is the chirp duration. IWRAP typically employs a 10 μs chirp length and either a 2

or 4 MHz chirp bandwidth resulting in a compression gain of 20 or 40 dB, respectively. While the previous equation for Z_{min} is shown without the added sensitivity of pulse compression, the following equation shows Z_{min} with the addition of pulse compression gain, $B\tau$:

$$Z_{min} = \frac{2^{10}(\ln 2)\lambda^2 R^2 l^2 l_r P_n}{\pi^3 P_t G^2 G_S \theta_1^2 c|K|^2} \times \frac{1}{B\tau}$$

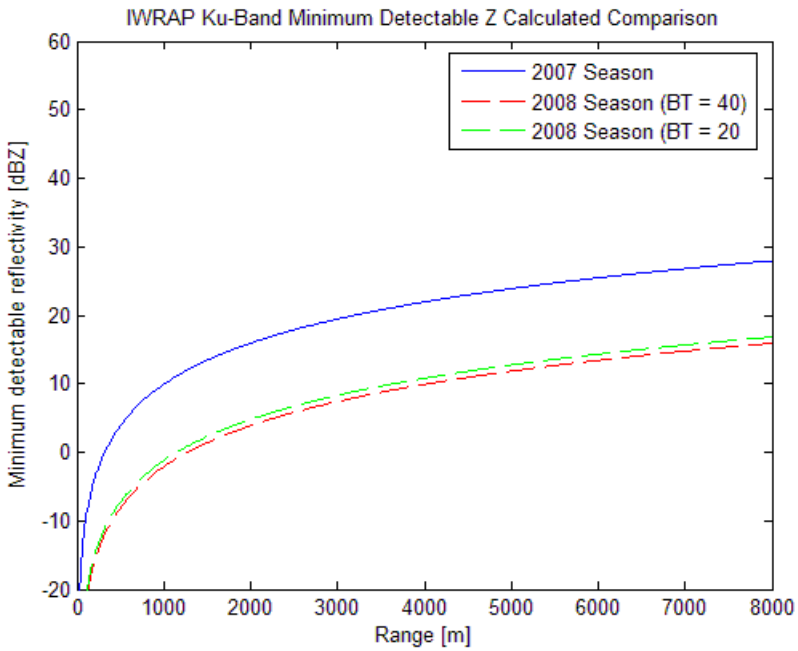

Figure 4.1. Calculated Comparison: Minimum detectable Z versus Range for Hurricane Seasons 2007 and 2008 (with varying pulse compression gains) at Ku-band

Figure 4.1 shows minimum detectable reflectivity for the 2007 season compared with the addition of pulse compression in the 2008 hurricane season. Notice the increase in sensitivity (of approximately 11-14 dB) with the addition of pulse compression compared to the previous pulsed system. A transmit power of 38 dBm (measured at the atenna) along with a noise power of:

$$P_n = kTBF = -100dBm$$

where k is Boltzmann's constant (1.38 x 10^{-23} J/K), T is temperature in Kelvin (nominally 290K), B is the receiver bandwidth (5 MHz), and F is the receiver noise figure (6.14 dB, improved prior to 2007 hurricane season).

4.2 Transmit Signal

The first step in implementing pulse compression in the IWRAP radar system was to decide which transmit waveform to use. Although nonlinear FM and phase-coded transmit waveforms offer better range sidelobe levels, a linear FM chirp was chosen for this application because it is a simple waveform to create.

Another benefit of using a linear FM chirp and pulse compression is that it acts as a filter, disallowing unwanted signals that do not possess the same frequency traits as the transmit signal from being detected. This proved to be beneficial in field experiments, as a radar operated by NOAA onboard NOAA-42 uses various C-band frequencies that were picked up by the IWRAP C-band radar while in pulse mode, but filtered out when pulse compression was used.

Range resolution must also be considered when designing a pulse compression radar system and a relevant transmit signal. For a pulsed radar, the range resolution is equal to:

$$\Delta R = \frac{c\tau}{2}$$

where ΔR is the range resolution (m), c is the speed of light (m/s), and τ is the pulse-length (s). For a pulse-length of 200 ns, this gives a range resolution of 30 meters. For a pulse compression radar system, range resolution is equal to:

$$\Delta R = \frac{c}{2B}$$

where ΔR is the range resolution (m), c is the speed of light (m/s), and B is the transmit signal bandwidth (Hz).

For the 2008 hurricane season, IWRAP was operated with a transmit bandwidth of either 2 or 4 MHz. This results in a range resolution of 75 meters (2 MHz) and 37.5 meters (4 MHz), respectively. These different bandwidths were chosen to keep the transmit bandwidth below the receiver bandwidth (5 MHz) to leave the option open for applying different post processing techniques. A 4 MHz chirp bandwidth was the primary transmit signal used for the 2008 hurricane season as it was desired to keep the range resolution as fine as possible.

4.3 Hybrid Transmit Waveform

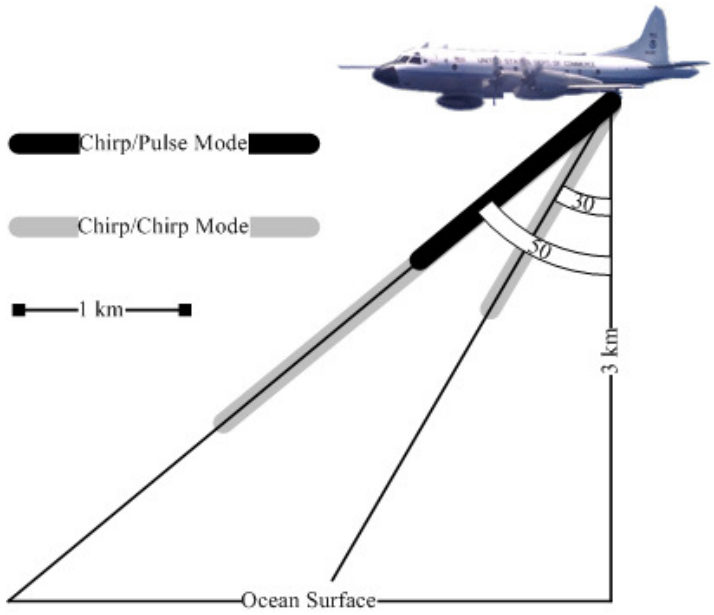

Figure 4.2. Diagram of the IWRAP blind-ranges for pulse/chirp and chirp/chirp modes. Note: the 30 meter blind range associated with a 200 ns pulse is not shown as the scale is too large.

For the 2008 hurricane season using a Hybrid Transmit Waveform (HTW) was suggested by Jim Carswell of Remote Sensing Solutions of Barnstable, MA. The idea was to create a transmit waveform consisting of linear FM chirps and unmodulated, fixed frequency pulses to simultaneously observe the short and far ranges [2]. An optimal HTW was designed and implemented by UMASS for the IWRAP radar system. This HTW consists of a 200 ns pulse at the lower incidence angle, and a 10 μs chirp (using pulse compression) at the higher incidence angle (pulse and chirp durations are easily altered). The reason for implementing the HTW is because range and pulse-length are adjustable parameters that effect the performance of the IWRAP airborne radar system, most noteably in high rain-rate situations.

Pulse-Length and Blind Range

The blind range of a radar is the range from an antenna in which a mono-static radar receiver is unable to sample, as it is in transmit not receive mode. This figure of merit is related to the pulse-length of the transmit waveform. This is an important factor to consider when creating a HTW because it effects how closely to the antenna a radar can sample. This is especially important in the case of IWRAP because it is an airborne radar system with a very limited altitude (range). Converting this amount of time to a range using the speed of light (c), we have:

$$BlindRange = \frac{c\tau}{2},$$

where τ is the pulse (or chirp) length. A diagram of the IWRAP blind-ranges for pulse/chirp and chirp/chirp modes is shown in Figure 4.2.

For the 2008 hurricane season, it was decided that a pulse-length for the longer range (higher incidence angle) of 10 μs was optimal. This leaves a blind range of 1.5 km at the 50^o angle, and a blind range of 30 m at the 30^o angle for the chirp/pulse mode. It was also decided that with the longer range associated with the higher angle,

the added average power (hence increased sensitivity) available with the use of pulse compression would be necessary only at the higher angle.

4.3.1 DDS

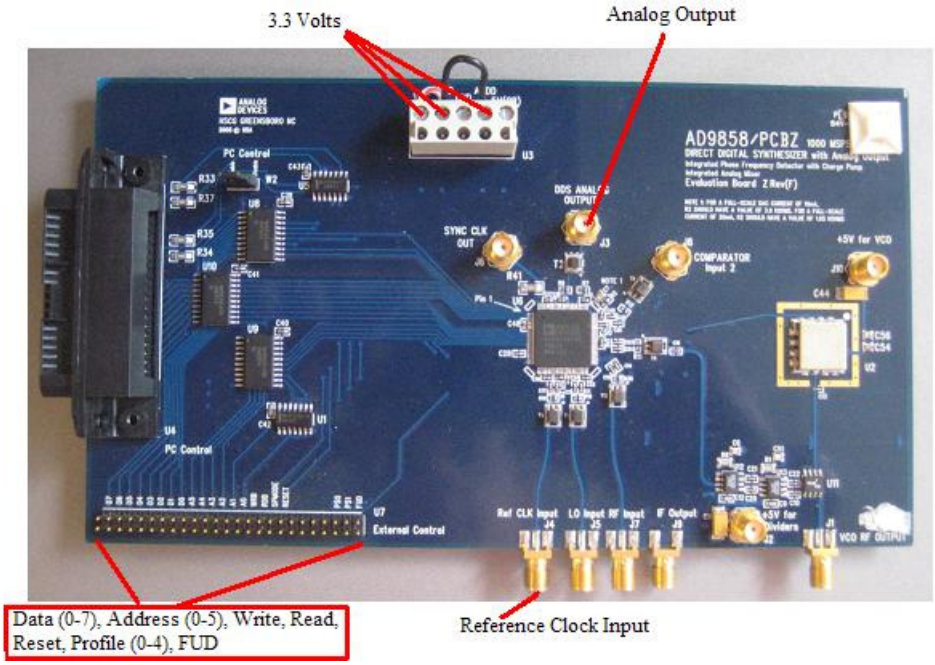

Figure 4.3. Analog Devices Direct Digital Synthesizer (DDS) Inputs and Outputs

The Analog Devices AD9858 DDS seen in Figure 4.3 was chosen to create the linear FM chirp for its frequency sweeping capability. This DDS automates much of the task of creating a chirped radar making it ideal for the pulse compression application. The DDS creates a frequency sweep by using a frequency accumulator, which repeatedly adds an incremental frequency to a start frequency. This causes the frequency to change with time, creating a chirp. The DDS requires 3.3 volts, which it receives from the aforementioned voltage regulator located on the FPGA buffer PCB. As previously mentioned all necessary input data used to program the DDS come from the FPGA, and the only ouput is either a single-tone at 30 MHz or a chirp

(of chosen bandwidth) centered at 30 MHZ. Appendix B explains how the DDS is programmed.

4.4 Received Signal Processing

Advanced filtering and windowing methods are required to compress linear FM signals on the receive end of a pulse compression radar system. Depending on the methods used to compress the received signal, various range sidelobe levels appear which affect the power measurements at their respective ranges. This is less important when observing a point-target, but IWRAP is used to measure volume reflectivity so range sidelobe levels are of significant importance. For this reason, several different filtering and windowing methods were investigated in an attempt to reduce range sidelobe levels as much as possible. Although some techniques used to compress received signals can be done using hardware before the signal is digitized, both techniques investigated here were done after A/D conversion via software processing.

4.4.1 Conjugate Matched Filter Method

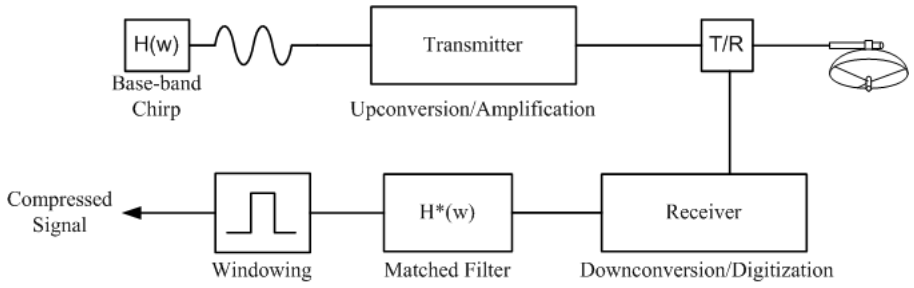

Figure 4.4. Diagram of the conjugate filtering technique. $H(\omega)$ represents the chirp centered at 30 MHz, while $H^*(\omega)$ is the complex conjugate. The windowed, compressed signal is the desired output.

A pulse compression radar is a practical implementation of a matched filter system [13]. A common matched filtering technique, and one that was used for pulse compression in the IWRAP real-time display, is the conjugate matched filter method.

The output of the matched filter is the compressed pulse, which is given by the IFFT of the received signal $H(\omega)$ multiplied by the matched filter response $H^*(\omega)$ (see Figure 4.4).

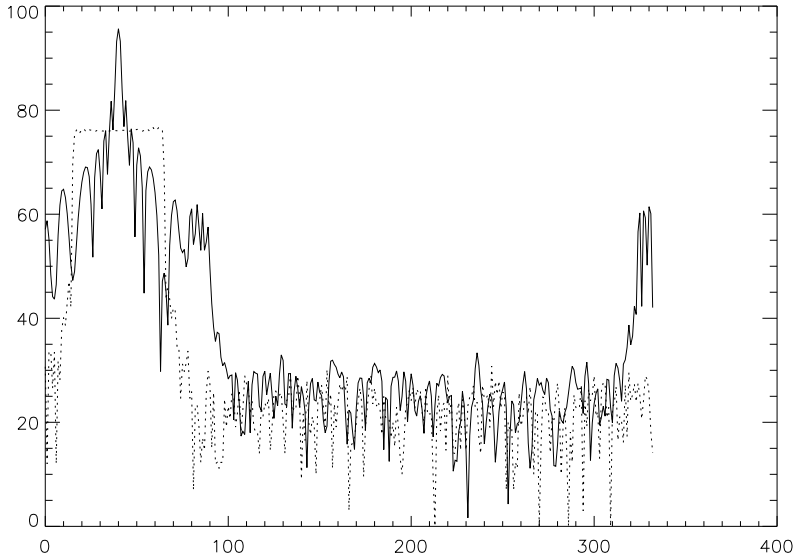

Figure 4.5. Output of the matched filter for 2 MHz bandwidth showing power (dB, y-axis) versus range bin (x-axis). The dotted line represents a power plot of the raw data before pulse compression.

In this case, the reference signal comes from the calibration loop in the form of a 50-point sequence of raw data containing the transmit FM chirp. Figures 4.5 and 4.6 show the output of the matched filter compared to the raw data for both 2 and 4 MHz at Ku-band. These plots show one PRI on the X-axis (333 samples @ 5 MHz sampling rate and 15 kHz PRF), while the Y-axis shows unscaled power levels.

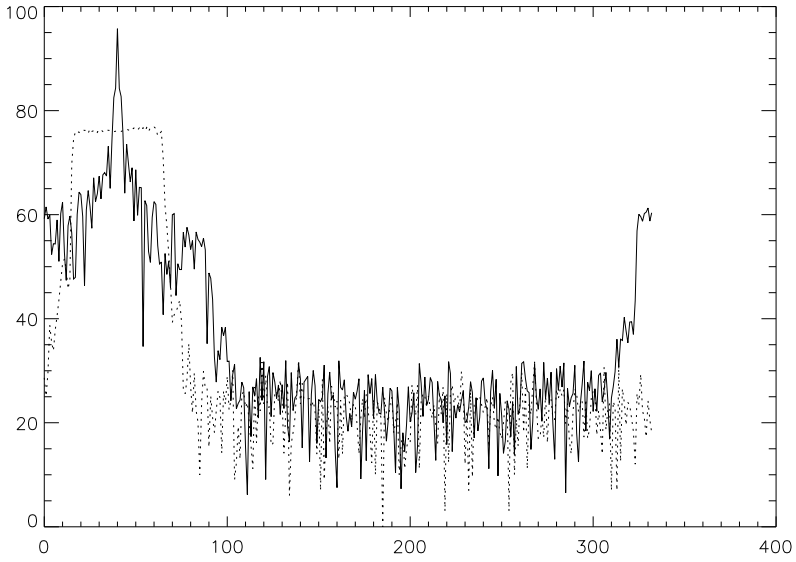

Figure 4.6. Output of the matched filter for 4 MHz bandwidth showing power (dB, y-axis) versus range bin (x-axis). The dotted line represents a power plot of the raw data before pulse compression.

4.4.2 Windowing Functions

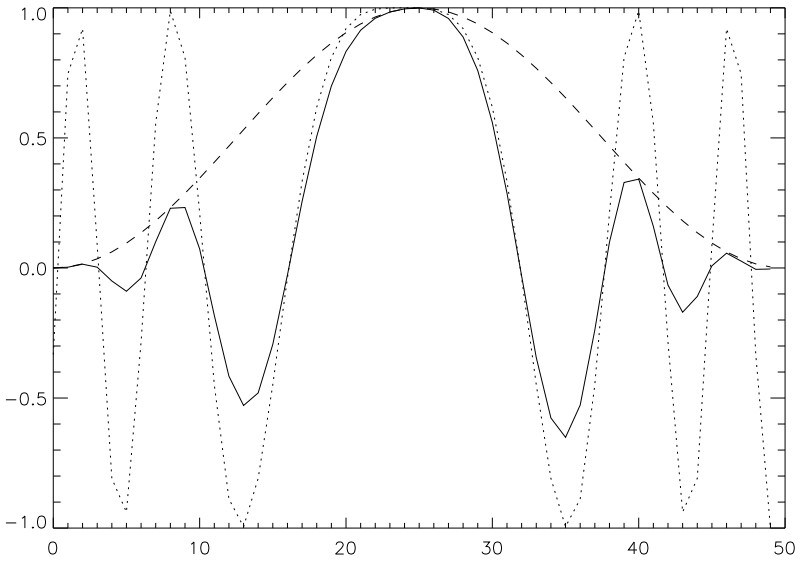

Figure 4.7. Plot of magnitude (y-axis) versus range bin (x-axis) showing the reference signal (dotted line), windowing function (dashed line), and windowed reference signal (solid line). The windowing function used here is a Hamming window.

Implementing a matched filter efficiently requires using an FFT based convolution technique. The FFT assumes that the finite interval over which the FFT takes place is one period of an infinitely long periodic sequence. This has the potential to introduce discontinuities when the end of the sequence does not match up with the beginning of the sequence (which is usually the case). To help limit these discontinuities a windowing function is applied to the signal in the time domain. This causes the signal to go to zero at the beginning and end of the time series, thus ensuring a smooth transition at either end of the sequence. Figure 4.7 shows the 50-point sequence of a 10 μs reference chirp with no windowing (dotted line), the windowing function (dashed line) and the signal after windowing is applied (solid line).

Weighting Function	Max Sidelobe Level (dB)	Loss of SNR (dB)	Width Spread of Mainlobe
Rectangle	-13.2	0	1
Hamming	-42.56	-1.34	1.41
Cosine-squared	-31.7	-1.76	1.62
Cosine-cubed	-39	-2.38	1.87

Table 4.1. Performance comparison of several windowing functions with respect to maximum sidelobe level, SNR loss, and added width of mainlobe. As can be seen in this table, each windowing function has a different effect on the signal it is applied to.

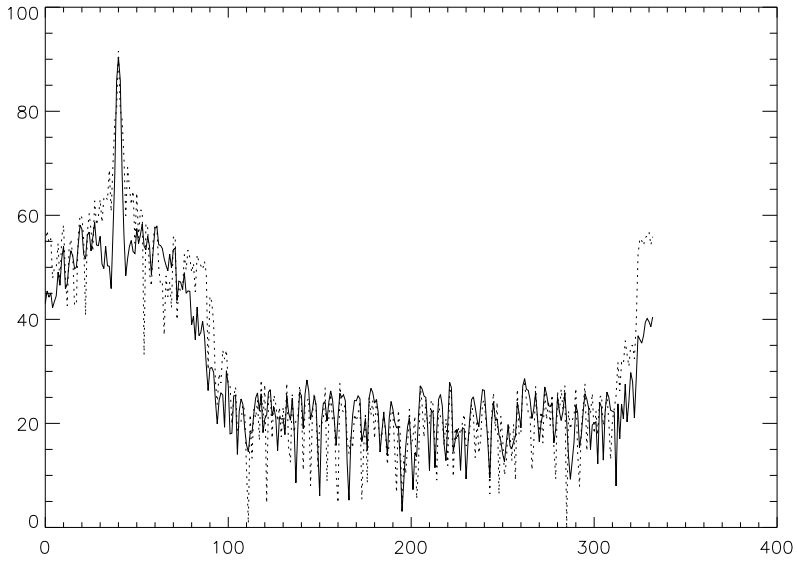

Figure 4.8. Plot of pulse compressed data using matched filtering with (solid line) and without (dotted line) applying a Hamming window. This plot shows power (dB, y-axis) versus range bin (x-axis) of 2 MHz bandwidth data.

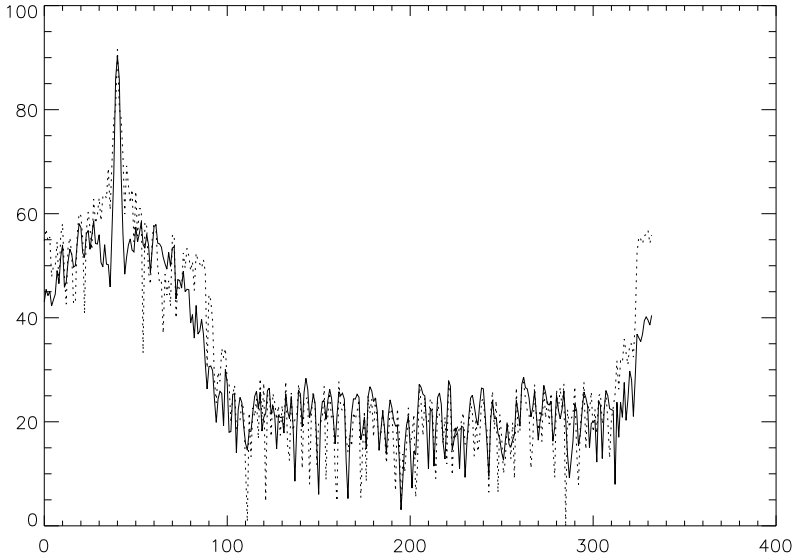

Figure 4.9. Plot of pulse compressed data using matched filtering with (solid line) and without (dotted line) applying a Hamming window. This plot shows power (dB, y-axis) versus range bin (x-axis) of 4 MHz bandwidth data.

Applying a windowing function to the matched filter helps reduce range sidelobes compared to the matched filter. Many different windowing functions can be used, with varying effects. Refer to Table 4.1 for a few examples.

Figures 4.8 and 4.9 show what the pulse compressed data looks like through matched filtering with (solid line) and without (dotted line) applying a Hanning window. In the following section, a more advanced filtering method is investigated in an attempt to reduce range-sidelobe levels during pulse compression.

4.4.3 Inverse Filter Method

A least-mean-square inverse filter was compared to a matched filter in the interest of range sidelobe suppression. This filter can act either directly on the received echo or on the output of the matched filter. For this case a filter is designed to act directly on the received echo. With this approach to pulse compression filtering, it is ideally required to use a digital filter which is inverse to the input data sequence. This means that the ideal response of the filter to the input data would be a sequence in which all the elements except one are zero [10]. This filter is designed by solving the discrete form of the Wiener-Hopf equation [1]:

$$R * \omega_o = p$$

where R is the auto correlation matrix of the input sequence, ω_o is the weighting sequence to be calculated, p is the discrete cross-correlation of the input sequence and the desired output sequence, and $(*)$ denotes convolution. The auto correlation matrix, R, is an example of a cyclic convolution matrix in which each row of the matrix is obtained from the previous row by a right-shift. The DFT of circulant matrices is directly related to the DFT convolution theorem, allowing the following equation to be solved using the convolution method:

$$R * \omega_o = p = FFT^{-1}[FFT(R) \times FFT(\omega_o)]$$

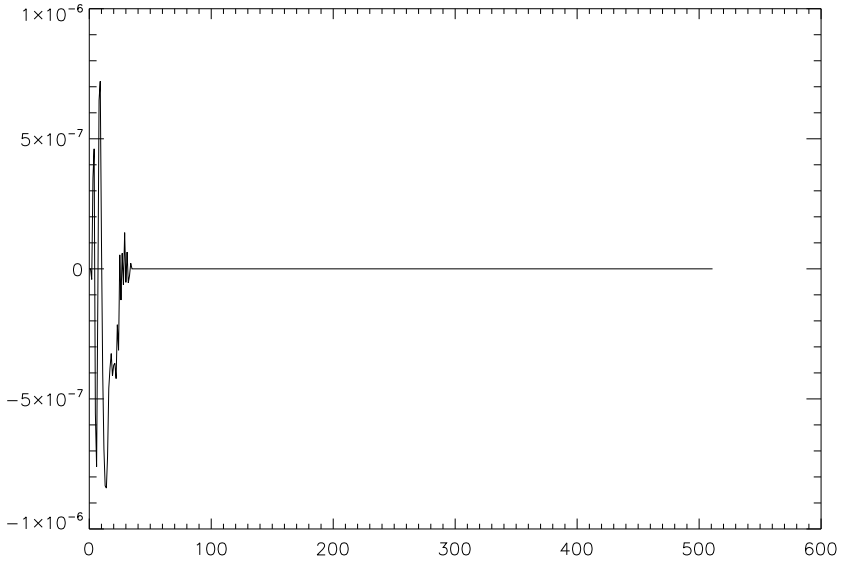

Figure 4.10. Plot of the weighting sequence used for inverse filtering showing magnitude (y-axis) versus range bin (x-axis)

The weighting sequence (ω_o) that results from the previous equation is padded with zeros to assure it is of adequate length before being applied to the received data. The weighting sequence is shown in Figure 4.10. The output of the filter shown in Figure 4.11 is obtained by taking the inverse FFT of the convolution of the input data and the filter weighting sequence:

$$CompressedData = FFT^{-1}[conj(FFT(\omega_o)) \times FFT(inputdata)]$$

The signal processing loss due to weighting is equal to:

$$Loss = \frac{\frac{(\Sigma\omega_o)^2}{\Sigma(\omega_o^2)}}{N}$$

where ω_o is equal to $\omega_o(N)$ and N is the length of the filter, in this case 33 points. For this filter design the loss due to signal processing is -0.579 dB, compared to -1.76091 dB for the hanning window.

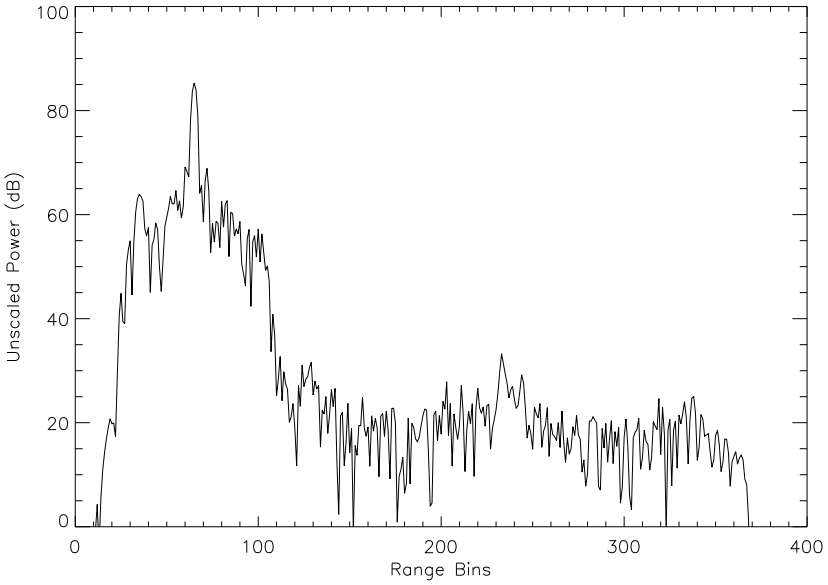

Figure 4.11. Output of inverse filter at Ku-band with a high rain-rate and 4 MHz bandwidth

Table 4.2 shows a comparison of loss due to weighting using an inverse filter compared to using a matched filter.

Filtering Method	**Max Sidelobe Level (dB)**	**Loss of SNR (dB)**
Matched Filter	-32 dB	-1.76091 dB
Inverse Filter	-17 dB	-0.579 dB

Table 4.2. Primary sidelobe level for both matched and inverse filters.

Since the auto correlation matrix (R) used in calculating the inverse filter is found using the raw data as an input, a filter designed using this approach will optimally compress the exact input sequence that was used to create the filter. It is helpful to

use an average of many sequences of input data in order to find a best fit calculation for R, but not always realistic with the high data rate associated with IWRAP. Using a best-fit value of R will create a filter that is effective in compressing a greater range of data. For best results the inverse filter should be recalculated periodically, most notably if the data changes significantly.

Another degree of freedom in constructing a filter capable of compressing a wide range of data is to adjust the filter length. This mitigates wrap-around effects but will inevitably raise the primary sidelobe levels. The inverse filter is beneficial in that it can be tailored almost endlessly depending on the desired output.

CHAPTER 5

FIELD TESTING AND DATA ANALYSIS

5.1 Field Testing Overview

While the initial system performance evaluation was conducted during short test-flights before the hurricane season, the majority of field testing occured while flying through eight different named storms throughout the 2008 hurricane season. The five hurricanes include Dolly, Gustav, Hanna, Ike, and Kyle while the three named tropical storms include Edouard, Fay, and Josephine. A typical hurricane reconnaissance mission lasts between 8 and 10 hours, and includes numerous storm penetrations. Data from both IWRAP radar subsystems, dropsondes, buoys, a C-band belly radar, an X-band Tail Doppler Radar (TDR), and SFMR collect data throughout missions. The QuickSCAT and ASCAT satelites collect data when passing over the storm systems as well. This data is collected to expand data sets, which in turn helps the different systems complement and calibrate each other. Data collected also helps to improve GMFs.

Because of typical storm track the highest winds in the storm usually located in the northeast quadrant, but this may not always be the case. For this reason the National Hurricane Center (NHC) will typically request a Figure-4 pattern in order to locate the strongest winds of the storm at the beginning of each hurricane reconaissance misson. The Figure-4 pattern starts by locating the plane at any of four corners of the storm, and flying diagonally through it. The plane then continues to one of the other two corners, and flies diagonally through the storm again. The flight plan is generally decided amongst scientists aboard the plane from there, depending

on different factors including wind strength, approaching land masses, storm track, etc.

Much of the data used in this thesis is from Hurricane Gustav. Gustav was the third hurricane of the 2008 atlantic hurricane season, and resulted in 138 confirmed deaths in the US and Carribean. Damage to the US from Hurricane Gustav totaled $15 billion, with an additional $3 billion worth of damage done to Cuba. The flight path of NOAA-42 from Hurricane Gustav on August 31^{st} is shown in Figure 5.1.

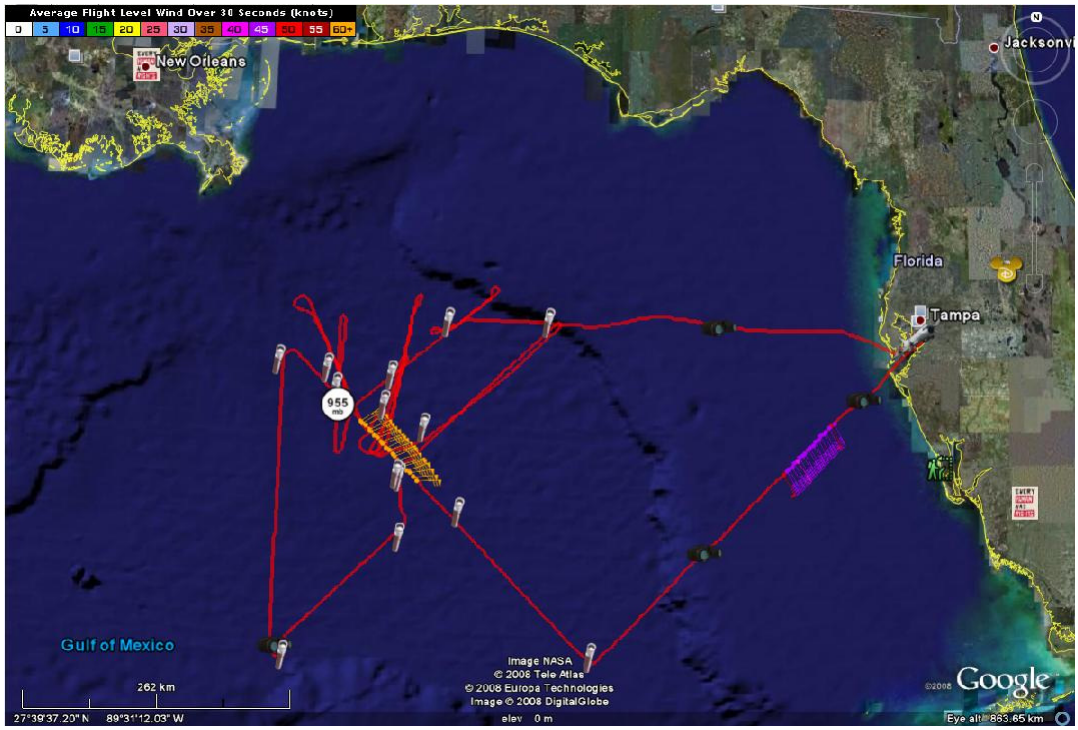

Figure 5.1. Global positioning data from NOAA-42 Gustav recon flight on August 31^{st} 2008. Dropsondes and buoy locations can also be seen throughout this map. (Photo courtesy of Google Earth and www.tropicalatlantic.com)

5.2 Data Analysis

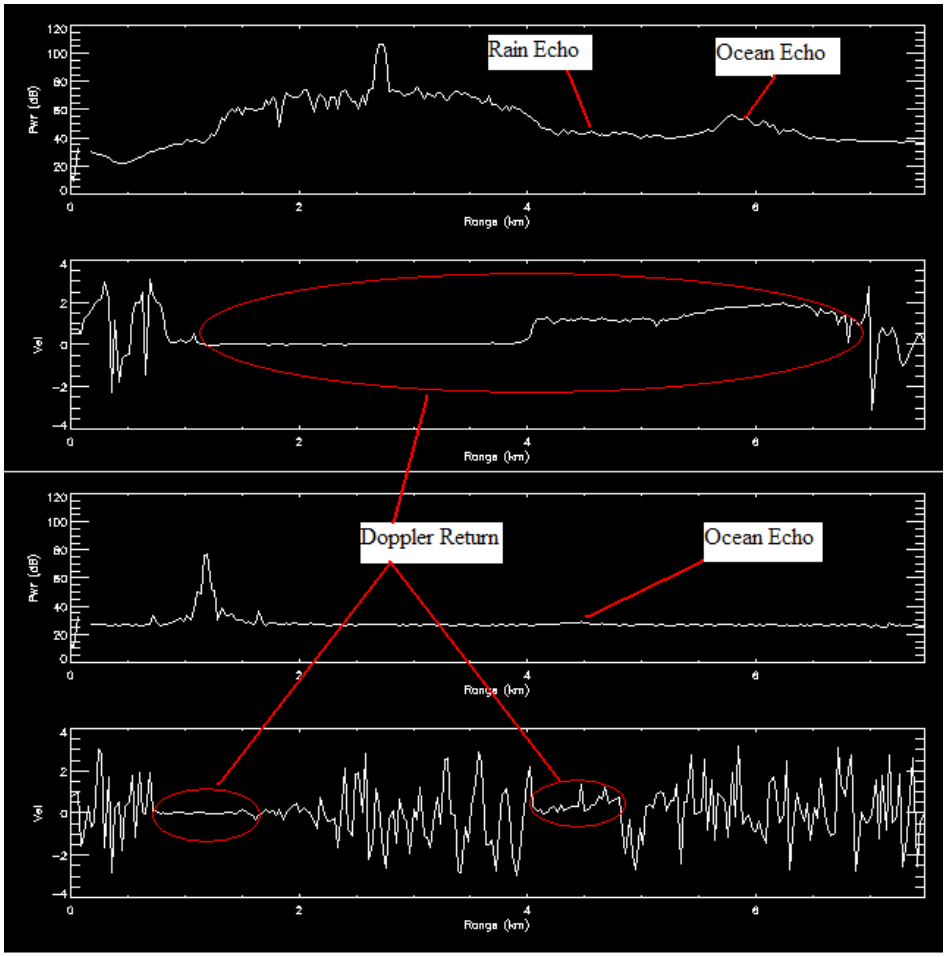

Figure 5.2. Pulse-pair power and velocity (unscaled) for Ku-band channel 1. Data is collected here to compare the compressed received echo of a chirp (top) and pulse (bottom). Notice the ocean surface echo is almost 'washed out' in the pulsed case, but not when pulse compression is used.

From August 29^{th} through September 1^{st} hurricane reconaissance missions were conducted as Hurricane Gustav traveled from the southeast of Cuba until it made landfall just west of New Orleans. IWRAP data was collected during these three missions with varying radar parameters to later compare their data sets. Most of the flights were conducted at 10,000 feet, however some were conducted at 7,000 feet as the Air Force reconaissance aircrafts typically claim airspace at 10,000 feet. For the

mission on the evening of August 29^{th} NOAA-42 flew at an altitude of 7,000 feet for this reason. This shorter range allowed IWRAP to be operated with a PRF of 20 kHz, instead of the typical 15 kHz. A quick view of the real-time display verified that a PRF of 20 kHz sufficiently captured the ocean surface echo while flying at 7,000 feet.

5.2.1 Chirp/Pulse Comparison

Data was collected at one point during Hurricane Gustav reconaissance flights in order to compare radar modes. During an eye wall penetration in a situation with a significant rain-rate, modes were switched less than 25 seconds apart in order to collect data using the pulse/pulse mode under the same weather conditions as with the chirp/pulse mode. Data was collected at an altitude of approximately 6500 feet, a PRF of 20 kHz, and a chirp bandwidth of 4 MHz. The pulse-pair data collected is shown in the real-time display seen in Figure 5.2 with both plots showing Ku-band channel 1. As can be seen in these plots, the surface echo is just about at the same level as the noise floor in the pulsed case, but rises approximately 20 dB above the noise floor when pulse compression is used. Looking at the Doppler plot for the pulsed case in Figure 5.2 notice that the circled data with discernable Doppler measurements are limited across the range, with the majority of the Doppler measurements looking like noise. This is because the return signal is below the noise floor. In contrast, Doppler measurements are visible across the full range when pulse compression is used. This easily verifies the increase in sensitivity (16 dB with a 4 MHz bandwidth, 13 dB for 2 MHz bandwidth) with the addition of pulse compression.

Channel 2 was also monitored during these high rain-rate situations in order to verify that the added sensitivity associated with pulse compression was not needed at the lower incidence angle. The range at this angle is significantly less (7500 feet at 30^o

incidence angle compared to 10,000 feet at 50^o) which directly effects the atmospheric loss through heavy rain.

5.3 Upgraded Control System Performance

Field testing of the control system proved that the improvements made to the IWRAP radar system made it much easier to run. Once the upgraded system was installed on the plane, the new calibration mode was very helpful as it eliminated moving switching controls via hardware, and allowed calibration to be easily done using the new GUI. Controlling the system with the new GUI and viewing the real-time display to verify functionality of the system was much easier than in previous seasons as it could all be done from Station 7. Network slowdowns, which previously required an operator to be sitting at Station 2 in front of one of the data acquisition computers, are now easy to detect by monitoring the real-time display from Station 7. The flexibility of the new control system allows the user to easily alter pulse-length or PRF depending on flying altitude, which was not an option before. All changes made to the system are now able to be easily and quickly analyzed by a user by simply opening the real-time display.

One notable problem found on an initial test flight was that once airborne and using the aircraft's 120 volt power system the FPGA input clock was lacking power. This was attributed to a possible lossy cable used on the plane that was not used while testing in the lab. Removing a couple dB worth of attenuation at the input to the FPGA reference clock alleviated this issue, but a malfunctioning FPGA was still considered. The problem did not arise again, but future flights were conducted with a spare FPGA on board.

CHAPTER 6

CONCLUSION

6.1 Summary of Work Completed

This thesis described the improvements made to IWRAP for the 2008 hurricane season. From January through July of 2008 much work was done to improve the IWRAP radar system. All software and hardware work done while redesigning the control system and adding pulse compression to IWRAP was done while keeping in mind the simplicity and dependability of an operational radar system. All unused hardware was removed where possible and the control system was completely rebuilt. The new control system design and computer interface make running the radar much easier, and the addition of pulse compression increases radar sensitivity and allows for the exploration of varied deployment scenarios. The new real-time display made it easy to troubleshoot problems during install and verify functionality of the system during deployments. Component boxes were consolidated while rebuilding IWRAP which saved space and weight while eliminating unnecessary points of failure associated with disorganized wiring.

Some difficulty arose in mounting the RAIDs and organizing the encoder bits for C-band, but these problems were solved within several days of discovering them (thanks to the help of past and present IWRAP contributors). There was also a small issue with the FPGA clock input being low, but this fix was as easy as removing an attenuator. The radar install went relatively smooth, and was succesfully completed prior to being tasked for any deployments.

Because of the 80 MB/s data-rate, halfway through the 2008 hurricane season the two 7+ TB RAIDs had to be swapped out for empty RAIDs. This was the only maintenance required by IWRAP throughout the entire hurricane season. Running the radar system was simplified to a point where a complete stranger to the system would be able to run it solo after just a few minutes of instruction. Data was collected on every mission N42 was tasked for during the 2008 season which resulted in approximately 25 TB of raw data.

At the conclusion of the 2008 hurricane season additional work was done in an attempt to lower range sidelobes through advanced filtering of the stored raw data. This inverse filtering technique compressed the received data, but resulted in greater range sidelobes compared to the matched filter approach. This being said, a compression filter created using the inverse filter method may prove to be useful in different radar systems with different filter designs.

6.2 Future Work

IWRAP will be called upon to participate in future hurricane seasons and may also deploy for winter wind experiments, traditionally based out of Alaska. Some IWRAP upgrades are mentioned below which would help verify different scatterometry techniques and demonstrate their potential benefit for the design of future systems.

Dual Polarization

In prior hurricane seasons IWRAP had been deployed as a dual-polarized radar system. This was done to be able to compare the scattering characteristics of the different polarizations with different storm conditions. This information is important for NOAA, JPL, NASA and the ESA, as they have interest in dual-polarization satelite-based scatterometer data that can be compared to IWRAP data at both

C- and Ku-band. This data is also important as these agencies will be considering different polarization schemes when designing future scatterometers.

For these reasons it will likely be desireable to convert IWRAP back to a dual-polarized radar system. The hardware and software improvements made to IWRAP for the 2008 hurricane season were completed with dual-polarization capability in mind. A few hardware upgrades will make it possible to convert IWRAP back to having dual-polarization capability; installing polarization switches, switching control signals, and a dual-channel rotary joint on the C-band spinner. Also necessary in the transition would be relocating the Ku-band front-end from the spinner back into the J-Cab.

New FPGA/DDS Board

Dr. James Carswell and his team at RSS have been working on a new FPGA/DDS board that will be able to be integrated into the IWRAP radar system in the future. This board will be able to generate all outputs needed for all radar control signals and triggers. This board will also be capable of transmitting a FM chirp with amplitude tappering to help combat range sidelobe levels. This board is in the testing stages at RSS, and a working prototype will be available to add to IWRAP in the near future.

APPENDIX A

QUARTUS BLOCK/SCHEMATIC SOFTWARE DESIGN

Refer to the schematic in Figure A.1 for all outputs and inputs that are explained in the following sections. Each block has an input clock, which is the 40 MHz clock going into the FPGA. Each block also has a reset, which is triggered when the user hits the 'STOP ALL' button on the IWRAP GUI.

UART Block

The UART block was developed by Jeung Joon Lee, and was freely obtained from the website www.cmosexod.com. As seen in Figure A.1 this block is the first of the FPGA block/schematic, and has inputs of a sys-clock, sys-reset, and rec-data. The two outputs are rec-data[7..0] and rec-ready. This block is designed to take the serial input data, and output it every clock-cycle as parallelized 8-bit packets. This block is the interface between the serial port and the main FPGA design.

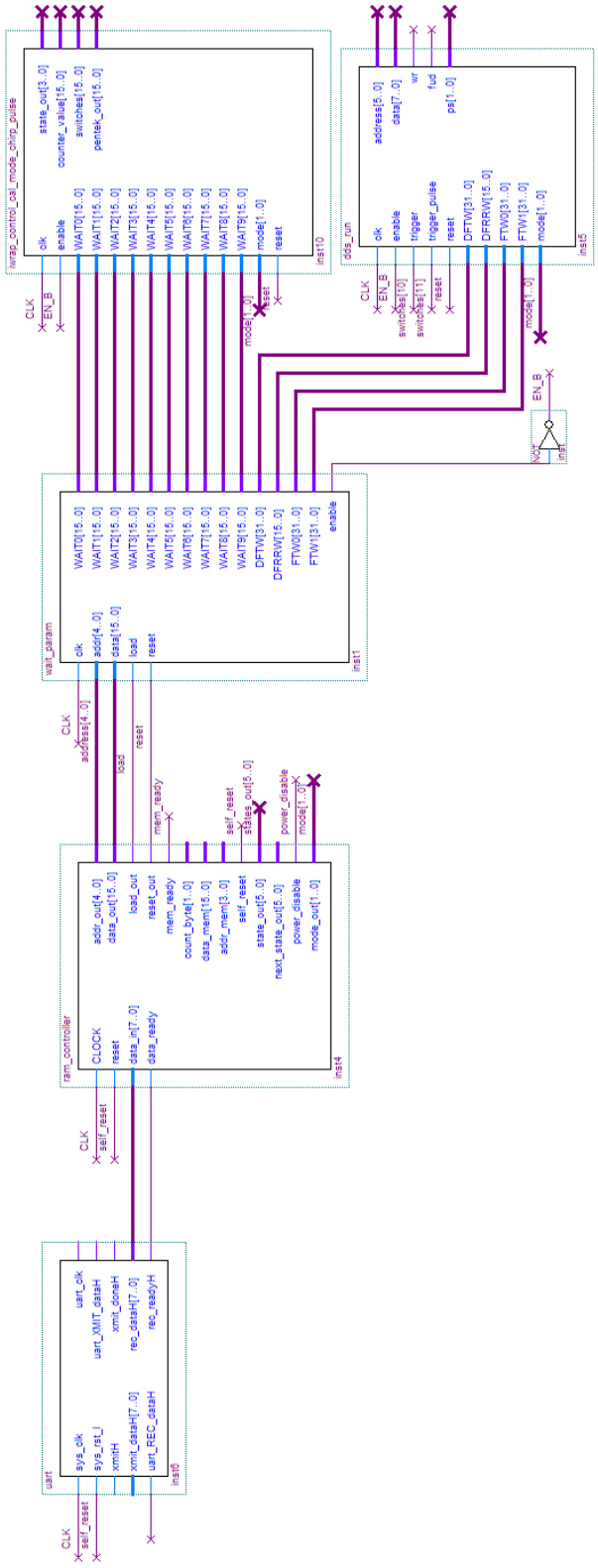

Figure A.1. FPGA Quartus block/schematic

RAM-Controller Block

Derived from code developed in October 2007 by Albert Genis, the final design of this block was developed with the help of Dragana Perkovic. The ram-controller block receives the parallelized data in 8-bit packets, and writes it to memory in 16-bit packets. Each 16-bit packet is then assigned an address, depending on its function (wait-states, DDS data blocks, and DDS mode). A state-machine then reads the memory blocks and loads it to the wait-param block. It takes two clock cycles (one to read, and one to load) for each 16-bit packet to be loaded to the next block (the wait-param block). This block also separates mode-out[1..0] output and sends one of four modes (pulse/pulse, pulse/chirp, chirp/chirp, and calibration) to the dds-run block.

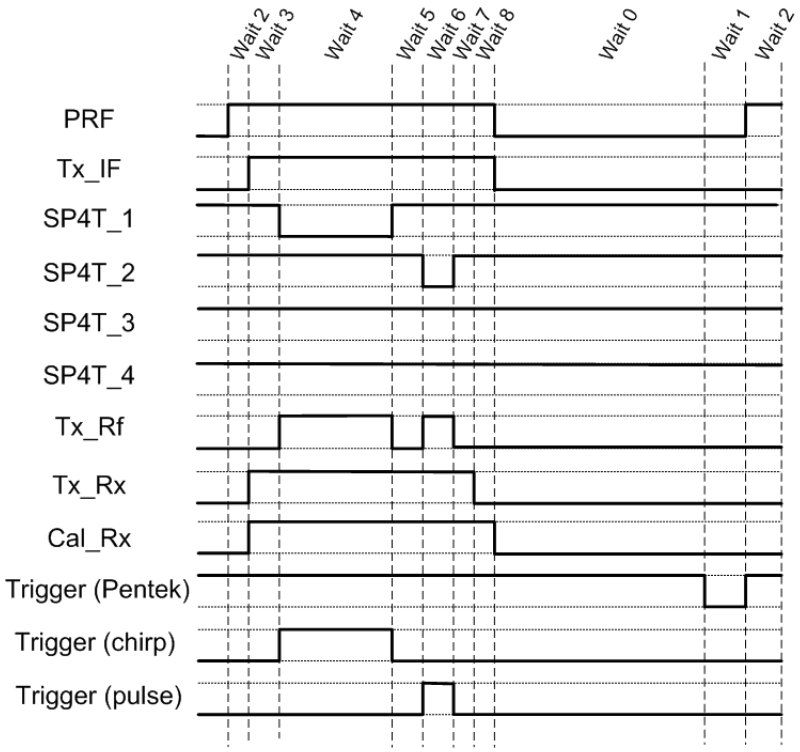

Figure A.2. Wait-states used for IWRAP timing and control signals for one PRI (not drawn to scale).

Wait-Param Block

FPGA Control Signal Outputs
PRF
TX-IF
SP4T-1
SP4T-2
SP4T-3
SP4T-4
Tx-RF
Tx-Rx
Cal-Rx
Trigger (Pentek)
Trigger (chirp)
Trigger (pulse)

Table A.1. IWRAP Control Signals. From the FPGA, these signals are sent to a PCB to be buffered, pulled-up to 5 volts, and split to be sent on to the corresponding C- and Ku-band radar systems.

Derived from code originally developed in May 2000 by J. Capdevila, this code was later altered by Dragana Perkovic and further by Albert Genis before being finalized for this IWRAP application. This block takes the 16-bit input data blocks, and organizes them into ten 16-bit wait-state blocks, three 32-bit and one 16-bit DDS programming data block. This block outputs all wait-states to the IWRAP-control-cal-mode-chirp-pulse block, and all DDS data blocks to the DDS-run block.

Note: Ten wait-states are seen here (compared to the nine seen in Figure A.2) because (1) a delay was needed as the DDS does not react quickly enough to the FPGA trigger and (2) it is necessary to trigger the Pentek low every few PRFs as it can not run at a 100% duty cycle.

IWRAP-Control-Cal-Mode-Chirp-Pulse Block

This block generates the real-time control signals that are sent to the 40-pin outputs on the FPGA. As an input it takes the ten 16-bit wait-state data packets as well as the 40 MHz clock. This block calculates all wait-states from the 16-bit wait-state data packets, and outputs either a 1 or a 0 (for high or low) for each control signal shown in Table A.1 resulting in the timing diagram seen in Figure A.2. For each control signal, a value of either 1 or 0 is held until the wait-state concludes, creating a timing scheme. This block runs through the each of the wait-states in order. The fastest time between states is a minimum of twice the input clock period, meaning the shortest delay, pulse-width, or trigger is 50 ns long.

DDS-Run Block

The DDS-run block outputs all data needed to program the DDS. While the actual programming of the DDS is explained in Appendix B, the process of writing data to the DDS registers is explained here. For inputs the DDS-run block takes three 32-bit data blocks (DFTW, FTW0, and FTW1) and one 16-bit data block from the wait-param block (DFRRW), reads, and stores the data into 8-bit memory blocks at assigned addresses, which are hard-coded values. These 8-bit data blocks are then written and loaded in parallel to the corresponding DDS registers. Once all the DDS registers are loaded, the DDS waits for a trigger from the IWRAP-control-cal-mode-chirp-pulse block. Once the DDS-run block receives the trigger, it will reset the frequency accumulator on the DDS and load the profile that was chosen in the GUI (to ouput either a pulse or a chirp).

APPENDIX B

DDS PROGRAMMING

This appendix explains how the different tuning words are calculated in order to program the DDS.

Delta Frequency Ramp Rate Word

The rate at which the frequency is incremented is set by the Delta Frequency Ramp Rate Word (DFRRW) register. This 16-bit value is set to one, which means the frequency will be incremented at the maximum rate which is 1/8 of the SYSCLK, or 125 MHz.

Delta Frequency Tuning Word

The frequency step size is set by the 32-bit Delta Frequency Tuning Word (DFTW) register. To calculate what value to use as the DFTW register, the following equation:

$$DFTW = \frac{BW \times 2^{35} \times DFRRW}{SYSCLK^2 \times CW}$$

is used, where CW is the chirp-width (s), SYSCLK is the input clock (Hz), and BW is the desired bandwidth of the chirp (Hz).

Frequency Tuning Word

The Frequency Tuning Word (FTW) is the 32-bit register where the start frequency of the chirp is loaded.

Register Name	Address Ser	Address Par	(MSB) Bit 7	Bit 6	Bit 5	Bit 4	Bit 3	Bit 2	Bit 1	(LSB) Bit 0	Default Value	Profile
Control Function Register (CFR)	0x00	0x00 <7:0>	Not Used	2 GHz Divider Disable	SYNCLK Out Disable	Mixer Power Down	Phase Detect PwrDwn	Power Down	SDIO Input Only	LSB First	0x18	N/A
		0x01 <15:8>	Freq. Sweep Enable	Enable Sine Output	Charge Pump Offset Bit	Phase Detector Divider Ratio (N) (see Table 10)		Charge Pump Polarity	Phase Detector Divider Ratio (M) (see Table 11)		0x00	N/A
		0x02 <23:16>	AutoClr Freq. Accum	AutoClr Phase Accum	Load Delta-Freq Timer	Clear Freq Accum	Clear Phase Accum	Open	Fast-Lock Enable	Don't Use FTW for Fast-Lock	0x00	N/A
		0x03 <31:24>	Frequency Detect Charge Pump Current (see Table 7)		Final Closed-Loop Charge Pump Current (see Table 8)			Wide Closed-Loop Charge Pump Current (see Table 9)			0x00	N/A
Delta-Freq Tuning Word (DFTW)	0x01	0x04	Delta Frequency Word <7:0>								–	N/A
		0x05	Delta Frequency Word <15:8>								–	N/A
		0x06	Delta Frequency Word <23:16>								–	N/A
		0x07	Delta Frequency Word <31:24>								–	N/A
Delta-Freq Ramp Rate (DFRRW)	0x02	0x08	Delta Frequency Ramp Rate Word <7:0>								–	N/A
		0x09	Delta Frequency Ramp Rate Word <15:8>								–	N/A
Frequency Tuning Word No. 0 (FTW0)	0x03	0x0A	Frequency Tuning Word No. 0 <7:0>								0x00	0
		0x0B	Frequency Tuning Word No. 0 <15:8>								0x00	0
		0x0C	Frequency Tuning Word No. 0 <23:16>								0x00	0
		0x0D	Frequency Tuning Word No. 0 <31:24>								0x00	0
Phase Offset Word 0 (POW0)	0x04	0x0E	Phase Offset Word No. 0 <7:0>								0x00	0
		0x0F	Not Used	Not Used	Phase Offset Word No. 0 <13:8>						0x00	0
Frequency Tuning Word No.1(FTW1)	0x05	0x10	Frequency Tuning Word No. 1 <7:0>								–	1
		0x11	Frequency Tuning Word No. 1 <15:8>								–	1
		0x12	Frequency Tuning Word No. 1 <23:16>								–	1
		0x13	Frequency Tuning Word No. 1 <31:24>								–	1

Figure B.1. AD9858 Register Map. Note the boxes in yellow (one clears the frequency accumulator, the other enables it). Both must be set high for the frequency sweep mode, else the DDS will output a single tone. (Photo Courtesy of Analog Devices)

$$FTW = \frac{F_{start} \times 2^{32}}{SYSCLK}$$

where SYSCLK is the 1 GHz DDS reference clock input (Hz) and F_{start} is the start frequency (in Hz).

All data required to load the DDS registers comes from the FPGA, more specifically the DDS-run block. A register map showing how the DDS registers are loaded is shown in Figure B.1.

To program the DDS, 8-bit packets of data are loaded (in parallel) into predetermined registers, whose addresses (also loaded in parallel) can be found in Figure B.1.

Each 8-bit packet of data and 6-bit packet denoting the address of the data packet destination consists of 1s and 0s, whose values are held high or low by the FPGA until written (these pins are located in Figure B.1 as D[0..7] and A[0..5]). Setting the WR-pin high, followed by the FUD-pin low writes the values into the registers on the DDS. This is done for each data packet that is needed to program the DDS. Once these values are loaded into the DDS registers, the DDS waits for a trigger that comes from the FPGA timing diagram. This trigger enables the DDS to output either a single tone or a chirp.

APPENDIX C

IWRAP GUI: DESCRIPTION OF USER INPUTS

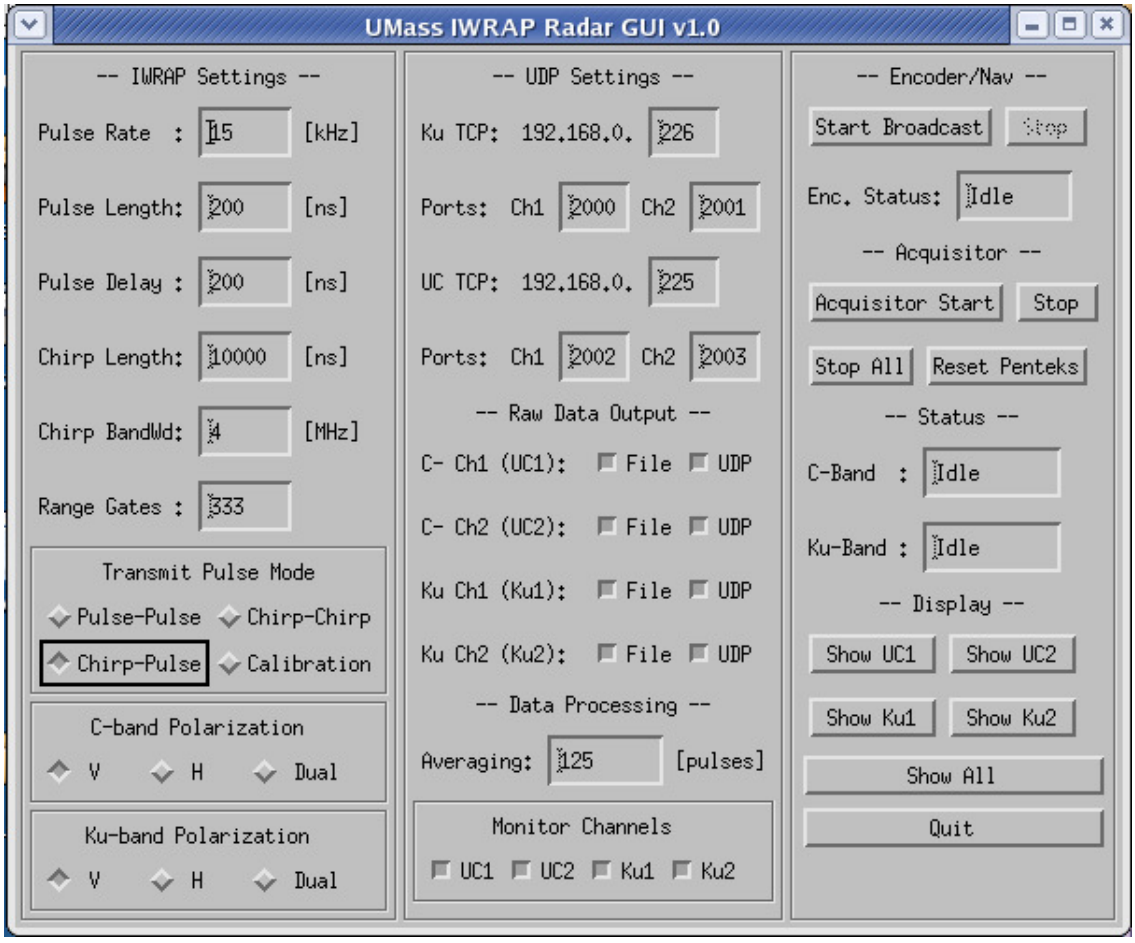

Figure C.1. IWRAP Radar GUI v1.0. The radar parameters seen in this GUI are the settings primarily used for the majority of the reconnaissance missions for hurricane season 2008.

The following list explains the different sections of the IWRAP GUI. A snapshot of the IWRAP GUI can be seen in Figure C.1.

- 'IWRAP Settings'- Here the IWRAP operator enters the main radar parameters, depending on the mission. The 'Range Gates' box is a calculated value not to be filled in by the user. There are 1024 range gates in a profile, and depending on the PRF a certain number of range gates will be used for each PRI. For the case seen in Figure C.1, 333 range gates are used for a PRF of 15 kHz. This means that three PRIs will fit in one profile, and the final 25 range gates in each profile will be thrown out in post-processing.

- 'Transmit Pulse Mode'- This part of the GUI lets the user decide on the radar mode of operation. Pulse-pulse mode was used in prior hurricane seasons, while the new calibration mode puts the radar system in a constant receive mode. This allows for ease in calibrating the receiver, while keeping any signal from being input to the high-power amplifiers to eliminate the possibility of damaging the high-power switches during calibration. The chirp/pulse mode was the primary mode used for hurricane season 2008, with the chirp being transmit first and at the higher incidence angle. Chirp/chirp mode uses pulse compression at both incidence angles, with a significantly increased blind range.

- 'C- and Ku-band Polarization'- In future hurricane seasons this section will be used to control the polarization switches (which have been removed for hurricane season 2008) for dual-polarization capability. Presently these buttons are used only to write into the header file which polarization is being used.

- 'UDP Settings'- This section allows the user to define which IP address each radar is using for data collection. For consistency reasons the Ku-band data acquisition computer (Desire) has an IP address of 192.168.0.226, while the C-band data acquisition computer (Fantasy) has an IP address of 192.168.0.225. These settings need not be changed under most circumstances.

- 'Raw Data Output'- Here the user can decide whether or not to collect data while running the radar. This is good for testing reasons, as it is not necessary to collect data when the aircraft is down and calibration/testing requires running the radar system.

- 'Data Processing'- This section applies to the pulse-pair data, which is saved to files on Beauty and is visible as the real-time display. This window allows the user to chose how many pulses are averaged for data collection.

- 'Monitor Channels'- This section allows the user to pick which channels are monitored. This is important for troubleshooting as it allows the user to independently monitor each channel to verify its performance. When all channels are working properly, all channels must be monitored to collect data for all channels.

- 'Encoder/Nav'- The Encoder/Nav 'Start Broadcast' button starts the nav stream (1 Hz aircraft data) and begins broadcasting the encoder data. This button must be pressed before the 'Acquisitor Start' button as to append encoder data to the files being created. The 'Enc. Status' shows if the encoder data is being broadcast (running) or not (idle).

- 'Acquisitor'- The 'Acquisitor Start' button starts the acquisitor program on both data acquisition computers, which starts data collection. The 'Reset Penteks' button resets the Pentek cards, which is necessary when the radar is first run after startup.

- 'Status'- As with the 'Enc. Status' window under the Encoder/Nav section of the GUI, the C-band and Ku-band status windows show if either radar is up (running) or not (idle).

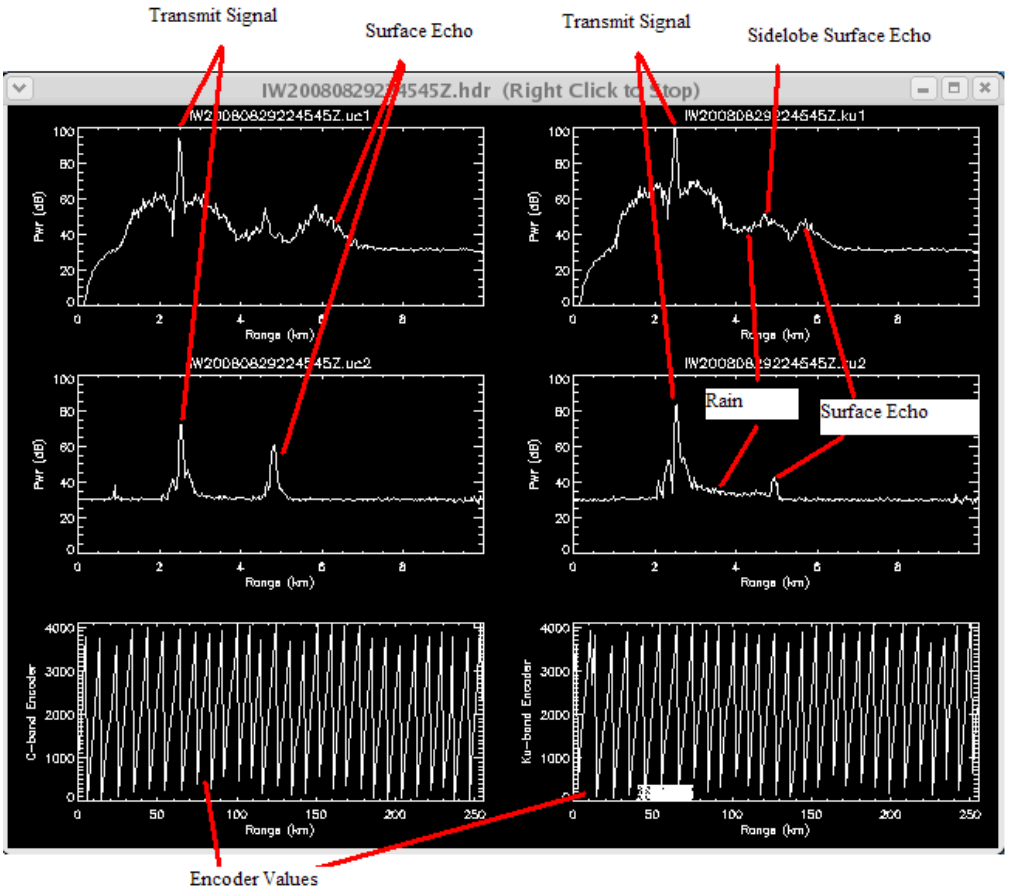

Figure C.2. IWRAP real-time display. C-band is the left-hand column, Ku-band is on the right. The higher incidence angle which uses pulse compression (channel 1) is located above the lower incidence angle (channel 2).

- 'Display'- This section is for the user to view the real-time display. Clicking on one of the 'Show XXX' bottons will show the calculated power levels of the pulse-pair data being collected on that channel, as well as the doppler frequency shift. Clicking the 'Show All' button will display all four channels, as well as both encoder outputs, as seen in Figure C.2.

APPENDIX D

TRANSMIT POWER LEVEL DOCUMENTATION

Transmit power was measured on with IWRAP installed on the aircraft as to eliminate as many unknown losses as possible. Table D.1 shows the peak output power for all four channels. Measurements were made using an Agilent N1911A power meter after a 50 dB high-power attenuator (M/N: 50HF-030-25/18S). For the 2008 hurricane season the encoder values for antenna position oriented towards the front of the aircraft were 2624 (C-band) and 594 (Ku-band).

Output Channel	**C-band**	**Ku-band**
Channel 1	42 dBm	42 dBm
Channel 2	38 dBm	42 dBm

Table D.1. Output power, C-band measured going into top of spinner, Ku-band measured going into antenna. These measurements were made on 9/29/08 before de-install.

APPENDIX E

OPERATORS GUIDE

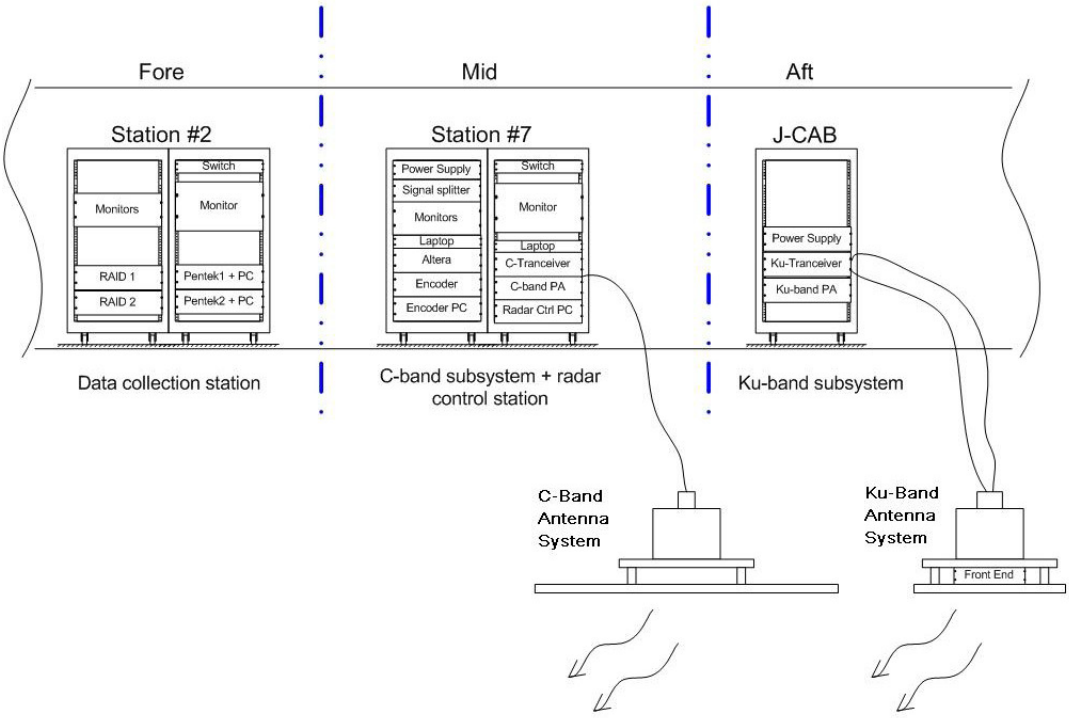

Figure E.1. Diagram of IWRAP radar component locations on NOAA-42 (diagram courtesy of Tao Chu). Note the Ku-Band front-end located on the antenna

This chapter is intended only to explain how to run IWRAP once the radar system is completely setup and working properly on the aircraft. It is not intended for troubleshooting, as an infinite number of issues can arise that may keep IWRAP from functioning properly. Refer to Figure E.1 for a view of the IWRAP system component layout.

- 'Uninteruptable Power Supplies (UPSs)'- There are two UPSs located towards the front of the aircraft. One is located on station 2, and that UPS powers the data acquisition computers. The second UPS is located behind the station 2 seat, in the station 3 rack. This is powered on from the back of the station 3 rack, and powers the two RAIDs. Aircraft power is cycled while starting up the engines (engine 2) which should be kept in mind when running any electronics on power that does not go through either UPS.

- 'Power-On RAIDs'- Just below the UPS on the back of station 3 are the power buttons for each RAID. They should be turned on prior to the data acquisition computers so the computers can mount them upon startup.

- 'Power-On Computers'- The four computers can be turned on next. While the computers can be turned on in any order, it takes the longest amount of time for Beauty to boot, so that should be kept in mind. The two data acquisition computers are located in station 2, while BigOther are located on the right side of station 7 along with Beauty.

- 'Power-On IWRAP Components- Station2'- While the computers are booting, the rest of the IWRAP components can be turned on. On the left side of station 7 the clock box, C-band power supply, and control box can be turned on. At this point the spinners can be set to the desired RPM.

- 'Power-On IWRAP Components- JCAB'- In the aft of the aircraft is the station known as JCAB. This houses the Ku-band power supply, front-end voltage distribution board, and high-power amplifier. The power supply can be turned on, and the left switch on the Ku-band high-power amplifier can be turned on to warm it up. The LEDs on the front will flash, and the 'Standby' LED will lighten up. Once the amplifier is warmed up, the LED will turn off.

- 'Log into Beauty'- When Beauty is up and running, log in by entering USERNAME: 'windman' and PASSWORD: 'mirsliwrap'.

- 'Open IWRAP GUI'- To get to the GUI, first open a command prompt, and change the directory to /data ($ cd data) and on the command line type 'iwrap' ($ iwrap). All fields in the GUI are explained in Appendix C.

- 'High-Power Amplifiers'- Once the radar is running the high-power amplifiers may be turned on. This is done for the C-band system by flipping the red rocker switch located on the C-band amplifier box on the right side of station 2. For Ku-band this requires going back to the JCAB and flipping the switch to the right on the Ku-band MPM box. The amplifier is on when the green LED illuminates. Now the radar is transmitting high-power, and the real-time display can be viewed to verify functionality of the radar system.

BIBLIOGRAPHY

[1] Ashod S. Mudukutore, V. Chandrasekar, Jeffrey Keeler. Pulse compression for weather radars. *IEEE Transactions on Geoscience and Remote Sensing, Vol. 36, NO. 1* (January 1998), 125–142.

[2] Carswell, James. Hybrid transmit waveform technique. Tech. rep., Remote Sensing Solutions, Inc., 3179 Main Street, Barnstable, MA 02630.

[3] Chu, Tao. Operation and improvement of the iwrap airborne doppler radar/scatterometer. Master's thesis, University of Massachusetts at Amherst, 2008.

[4] Daniel Esteban Fernandez, Xuehu Zhang, Antonio Castells David McLaughlin James Carswell Paul Chang Laurence Connor Peter Black Frank Marks. The imaging wind and rain airborne profiler- a dual frequency dual polarized connically scanning airborne profiler radar. *0-7803-7929-2/03IEEE* (February 2003), 4246–4248.

[5] Daniel Esteban Fernandez, Elizabeth Kerr, Antonio Castells James R. Carswell Stephen J. Frasier Paul S. Chang Peter G. Black Frank D. Marks. The imaging wind and rain airborne profiler for remote sensing of the ocean and the atmospheric boundary layer within tropical cyclones. *IEEE Transactions on Geoscience and Remote Sensing 43* (August 2005), 1775–1787.

[6] Falcon, Peter. Missions-seawinds on quikscat. website: http://winds.jpl.nasa.gov.

[7] J. Figa-Saldana, J.J. Wilson, E. Attema R. Gelsthorpe M.R. Drinkwater, and sStoffelen, A. The advanced scatterometer (ascat) on the meteorological operational (metop) platform: A follow on for european wind scatterometers. *Canadian Journal of Remote Sensing* (2002), 404–412.

[8] James R. Carswell, Steven C. Carson, Robert E. McIntosh Fuk K. Li Gregory Neumann David J. Mclaughlin John C. Wilkerson Peter G. Black S. V. Nghiem. Airborne scatterometers: Investigating ocean backscatter under low- and high-wind conditions. *Procedings of the IEEE* (December 1994), 1835–1860.

[9] Laboratory, Jet Propulstion. Seawinds on quikscat level 3 daily, gridded ocean wind vectors (jpl seawinds project). *Physical Oceanography Distributed Active Archive Center* (October 2001).

[10] Martin H. Ackroyd, F. Ghani. Optimum mismatched filters for sidelobe suppression. *IEEE Transactions of Aerospace and Electronic Systems, Vol. AES-9, NO. 2* (March 1973), 214–218.

[11] Paul S. Chang, Laurence Connor, Zorana Jelenak. Ocean surface wind research and operations at noaa/nesdis/ora. Tech. rep., NOAA/NESDIS Office of Research and Applications, Camp Springs, MD.

[12] Simon H. Yueh, Bryan Stiles, Wu-Yang Tsai Hua Hu, and Liu, W.T. Quikscat geophysical model function for hurricane wind and rain. *0-7803-7031-7/01IEEE* (July 2001), 1089–1091.

[13] Skolnik, M.I. *Radar Handbook*, 2nd ed. McGraw-Hill, Boston, Massachusetts, 1990.